Rational Design of Mixed-Metal Oxides for Chemical Looping Combustion of Coal via Experimental and Computational Studies

Amit Mishra*

Nathan Galinsky

Arya Shafiefarhood

Erik Santiso (co-PI)

Fanxing Li (PI)

CBE
NC STATE
UNIVERSITY

04/19/2016

Outline

- Background

- Experimental investigation of $Ca_xA_{1-x}Mn_yB_{1-y}O_3$ based oxygen carriers

- Computational investigation of $Ca_xA_{1-x}Mn_yB_{1-y}O_3$ based oxygen carriers

- Selection criteria for commercially viable oxygen carriers
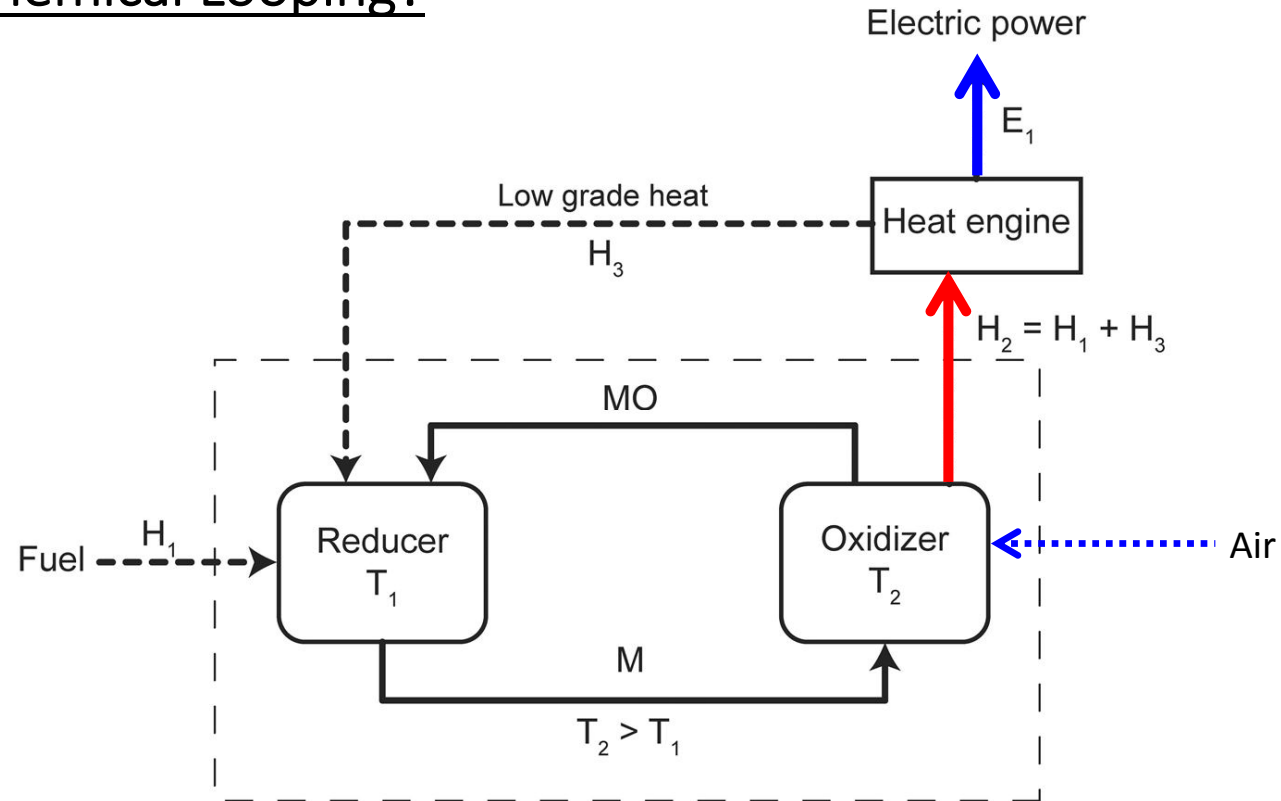
- Conclusions

A Closer Look at World Energy Projections
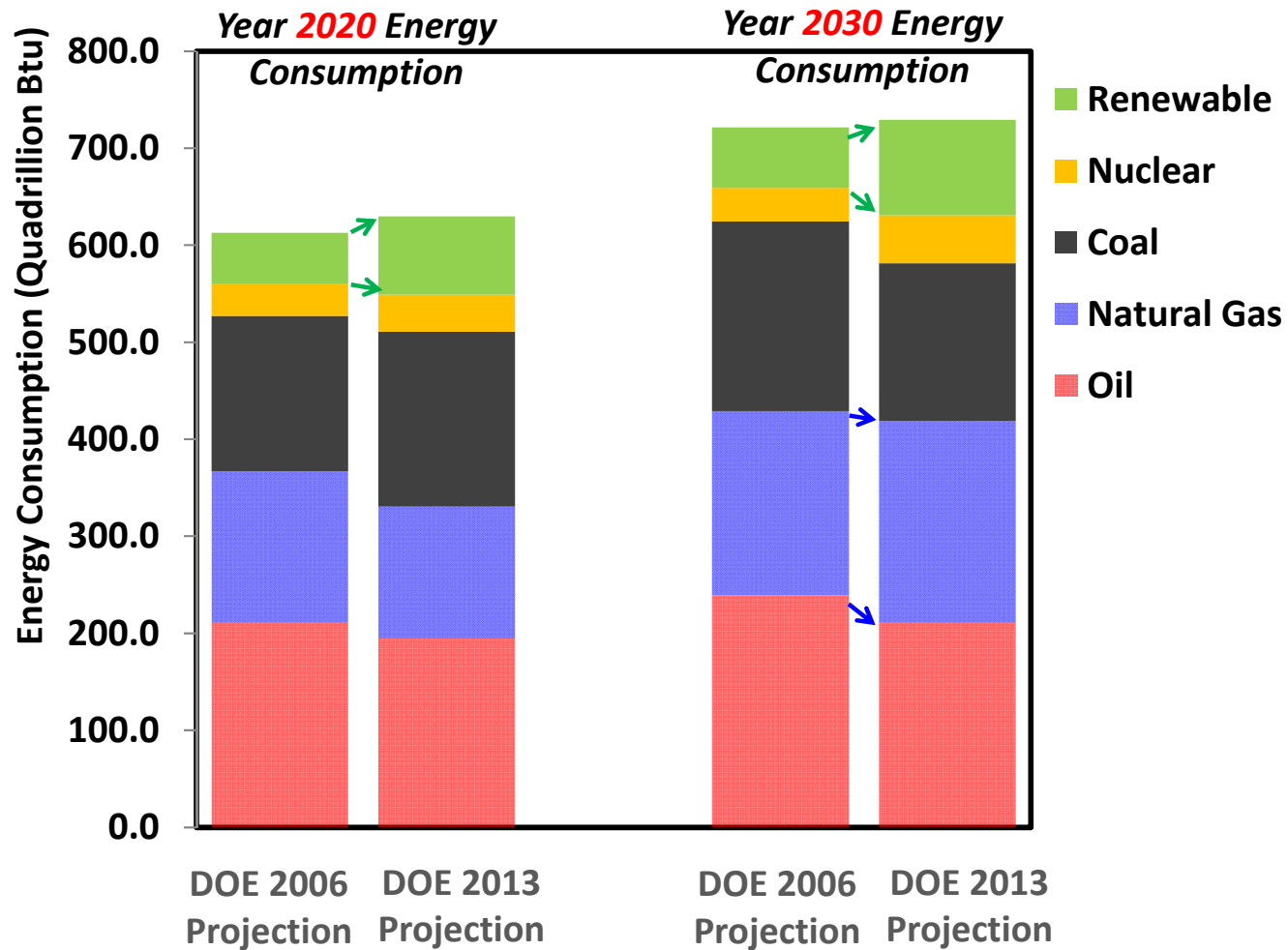
Carbonaceous Fuel Conversions via Chemical-Looping Combustion

H₂O/CO₂
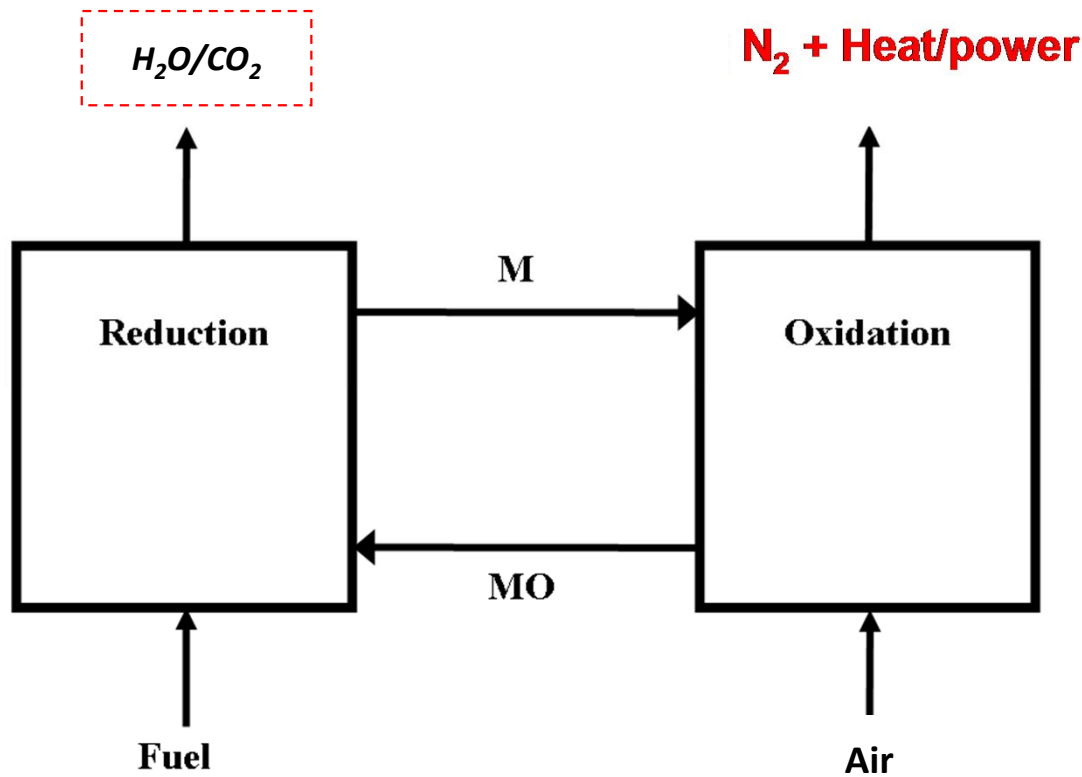
N₂ + Heat/power

- 2-Step Redox Loop
- Product: Heat, Power
- Integrated CO₂ Capture

Fan, L.-S. Chemical Looping Systems for Fossil Energy Conversion. Wiley, 2010.

Why Chemical Looping?

Electric power

E_1

Low grade heat

H_3

Heat engine

$H_2 = H_1 + H_3$

MO

Reducer T_1

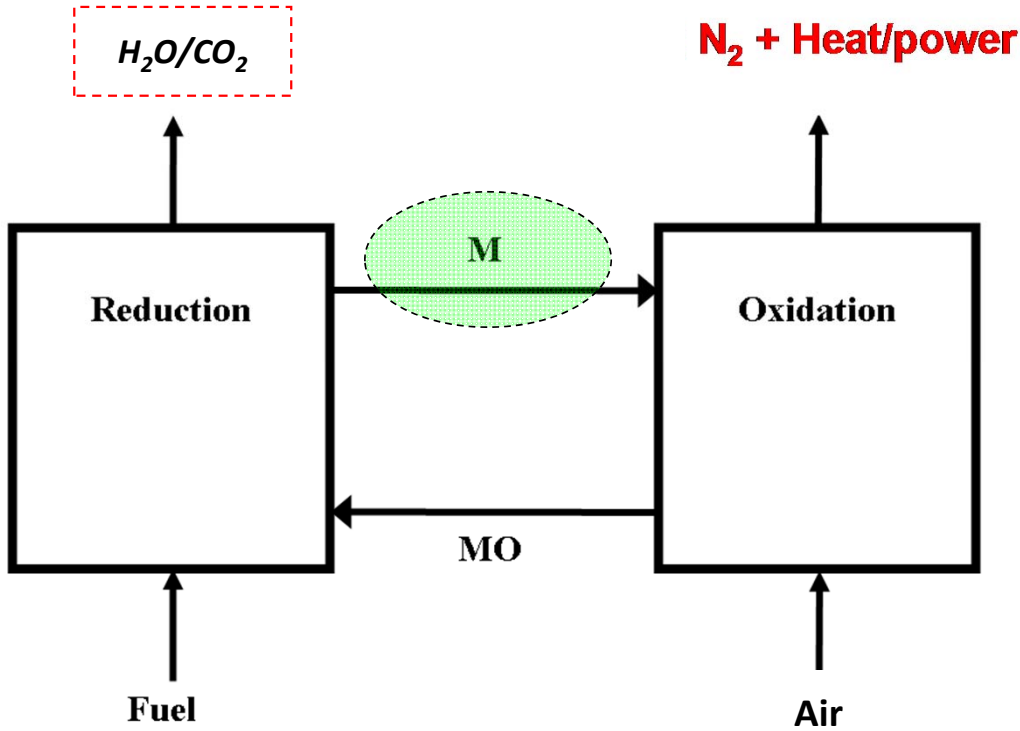Oxidizer T_2

Fuel H_1

Air

M

$T_2 > T_1$

Potential advantages of Chemical looping:

- **Tunable enthalpy extractible for heat engines through heat recuperation**
- **Fully integrated carbon dioxide separation cycle**
- **Delivery pressure of CO_2 can potentially be high**

High 2nd Law efficiency!

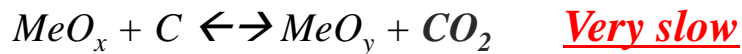# Chemical Looping Processes – Challenges

Keys Challenges:

1. _Reactor design_ that can effectively convert and circulate oxygen carrier particles
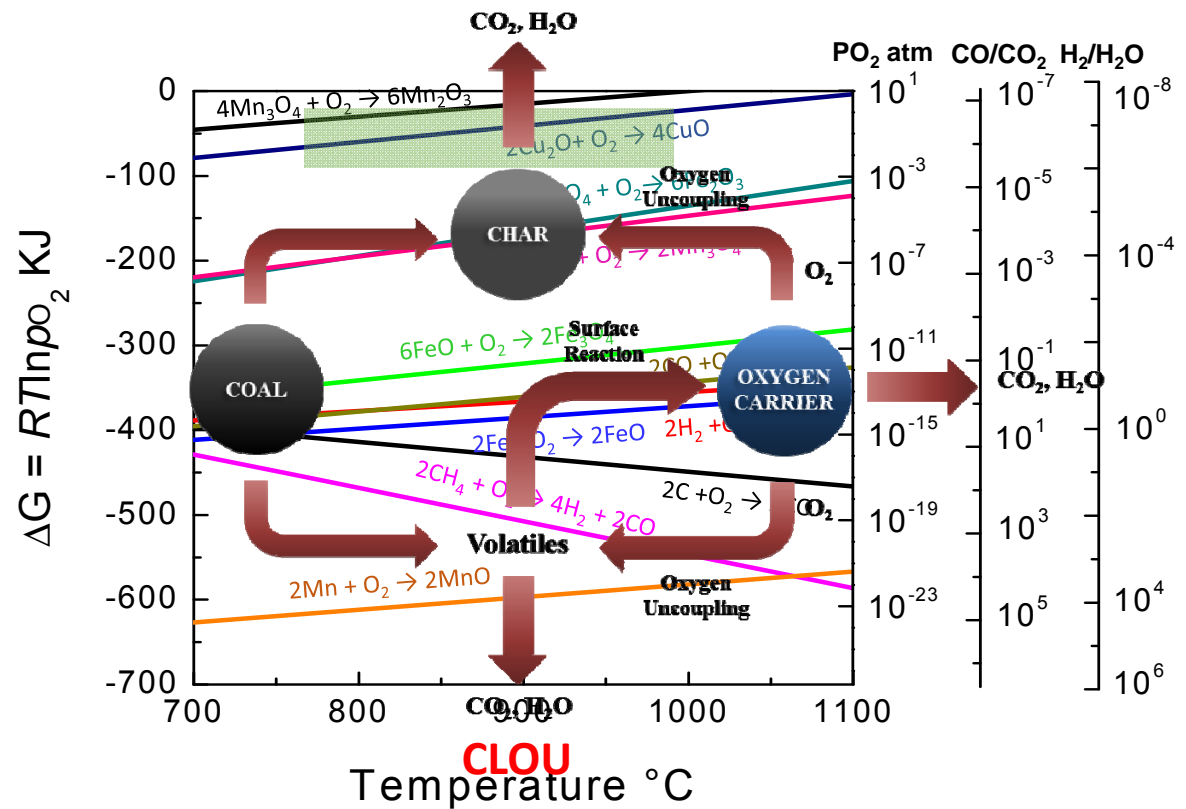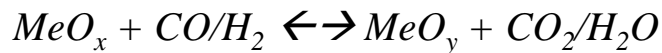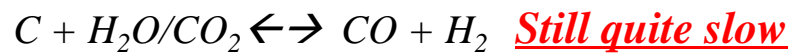2. **_Oxygen carrier particles_ with good reactivity, recyclability, and attrition resistance;**

Fan L-S. Chemical looping systems for fossil energy conversions. John Wiley & Sons, 2010

Chemical Looping Processes – Challenges and Opportunities <u>for Coal</u> Conversion

Challenge: Solid-solid reaction

$$MeO_x + C \longleftrightarrow MeO_y + CO_2 \quad \textbf{\textit{Very slow}}$$

Solution: In-situ gasification of solid fuel

$$C + H_2O/CO_2 \longleftrightarrow CO + H_2 \quad \textbf{\textit{Still quite slow}}$$

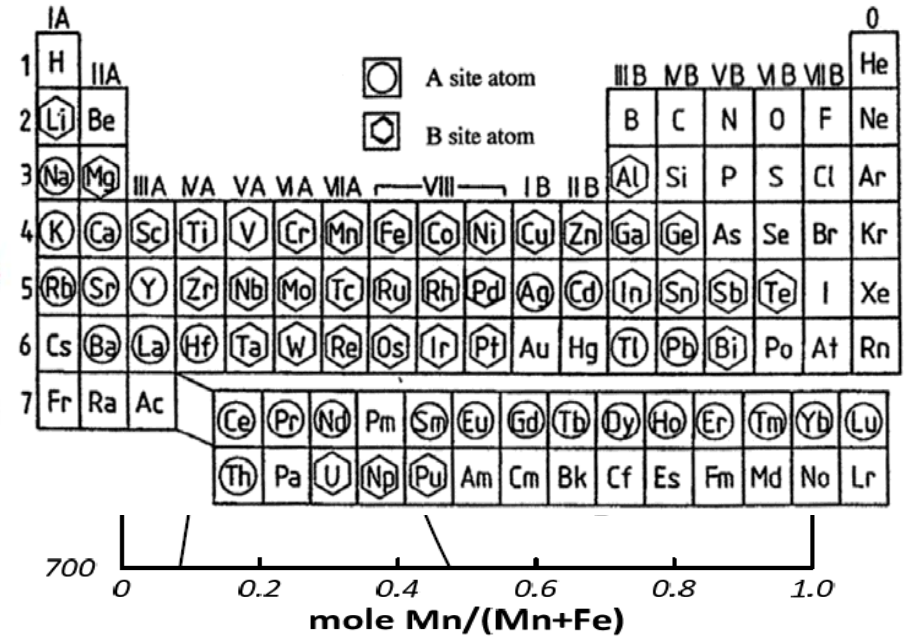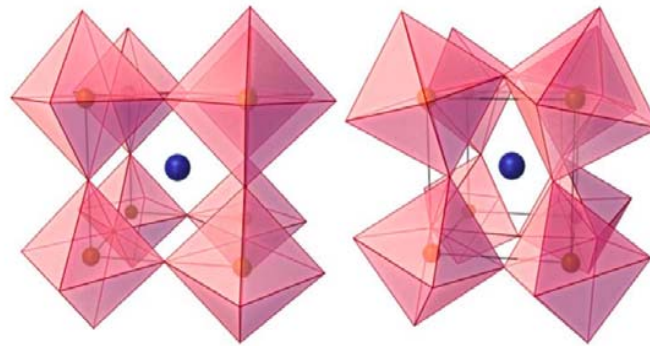$$MeO_x + CO/H_2 \longleftrightarrow MeO_y + CO_2/H_2O$$

Chemical Looping with Oxygen Uncoupling (CLOU) can be a potentially effective approach for redox based coal combustion

Material Selection – Rapidly Expanding Material Design Space
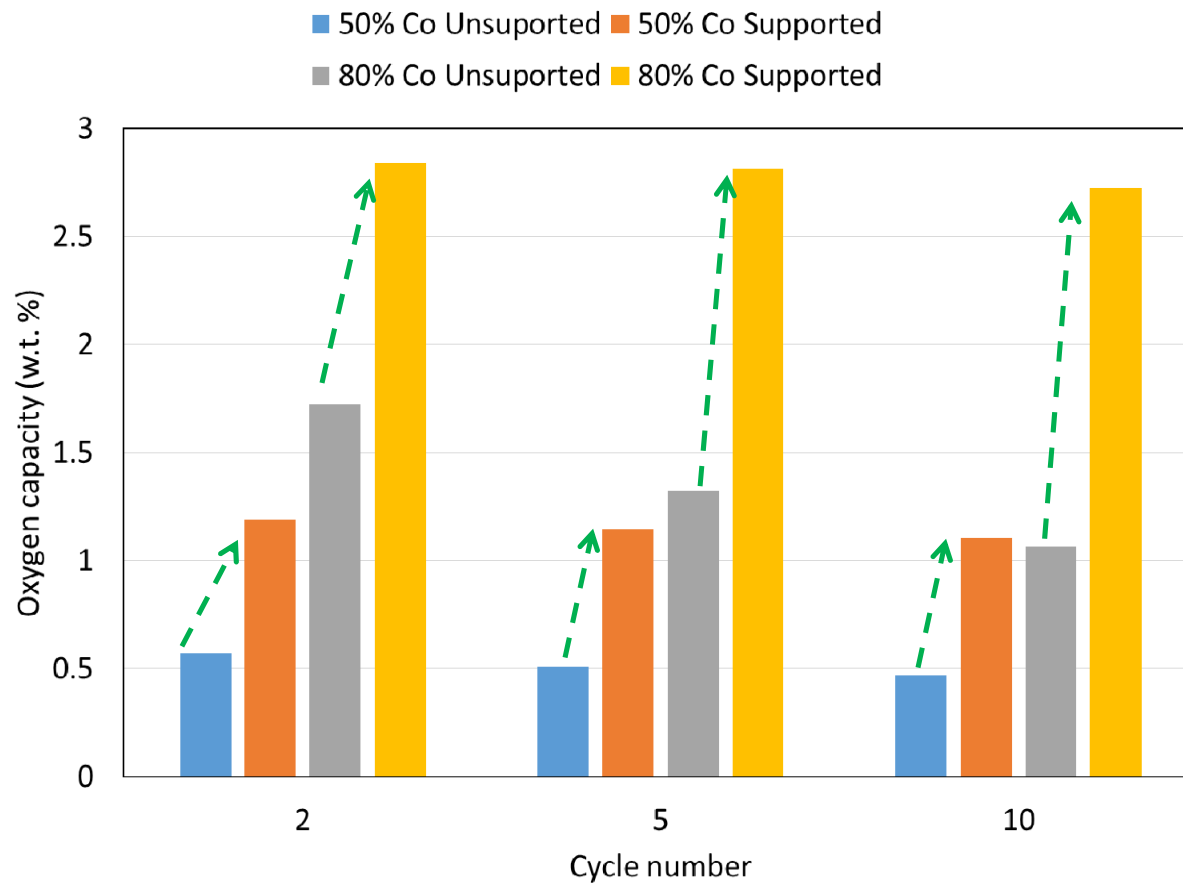
Oxygen carrier selections

- Iron
- Copper
- Manganese
- Nickel
- Cobalt
- Mixed first row transition metal oxides
- Perovskite materials

NC STATE UNIVERSITY

Perovskite Supported Fe-Co and Fe-Mn CLOU Carriers


850 °C, He inert ←→ 10% O$_2$

Up to 2.9 w.t.% oxygen carrying capacity achieved, supports significantly enhances the CLOU performance

Outline

- Background

- **Experimental investigation of $Ca_xA_{1-x}Mn_yB_{1-y}O_3$ based oxygen carriers**

- Computational investigation of $Ca_xA_{1-x}Mn_yB_{1-y}O_3$ based oxygen carriers

- Selection criteria for commercially viable oxygen carriers

- Conclusions
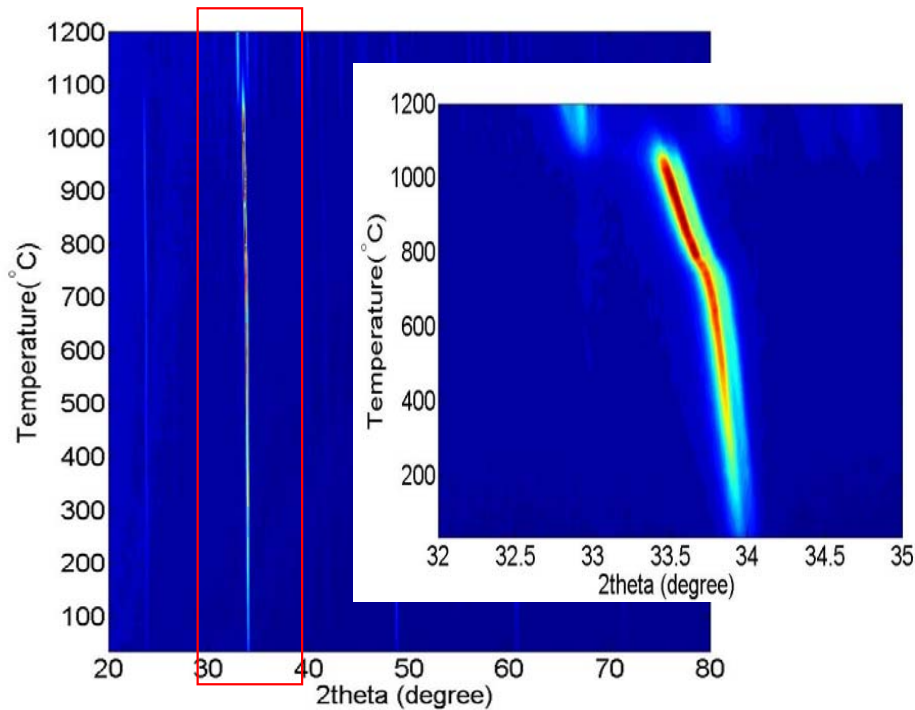
Stability Challenges for CaMnO$_3$: *In-Situ* XRD Studies
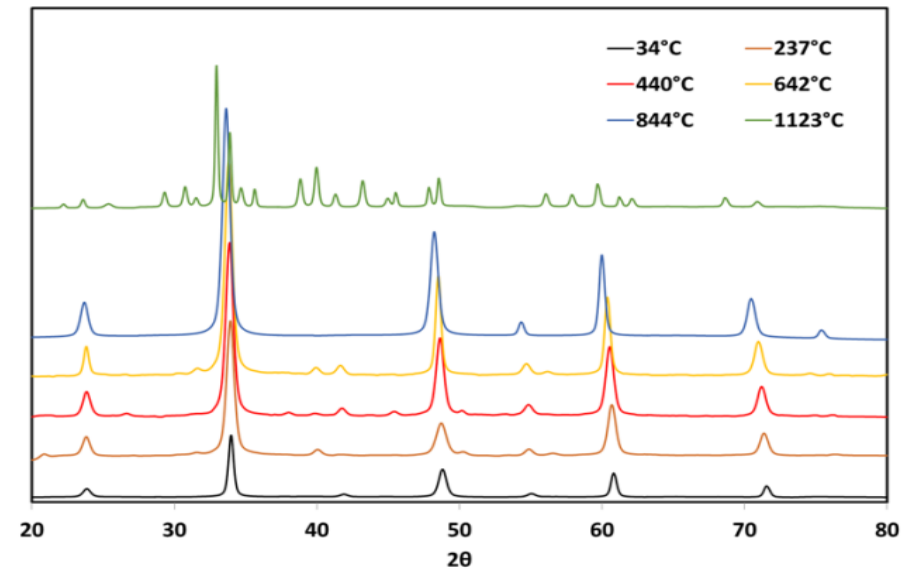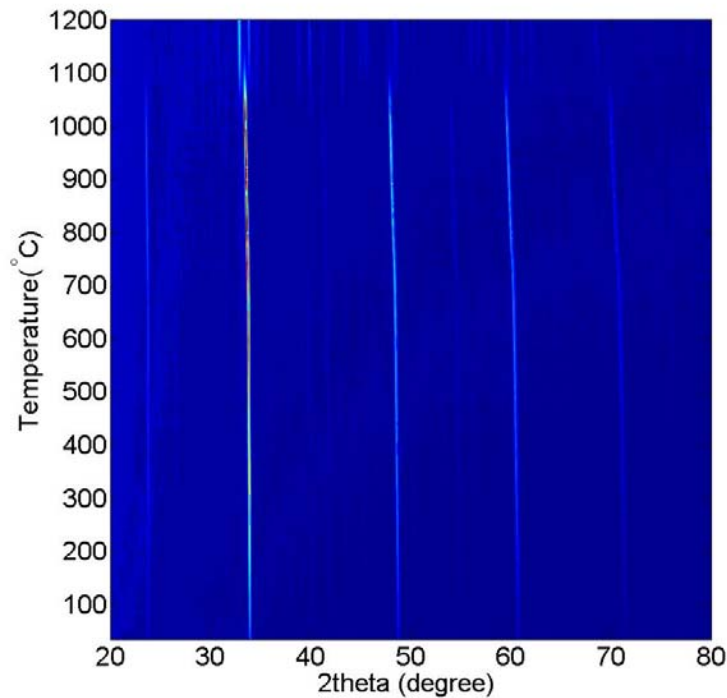
CaMnO$_3$ is chosen as the base material due to its well-known CLOU Properties
- Peaks begin to significantly shift between 800-850°C ; sign of oxygen uncoupling
- Up to 1100°C cubic CaMnO$_{3-\delta}$ remains stable

Stability of CaMnO$_3$: *In-Situ* XRD Studies
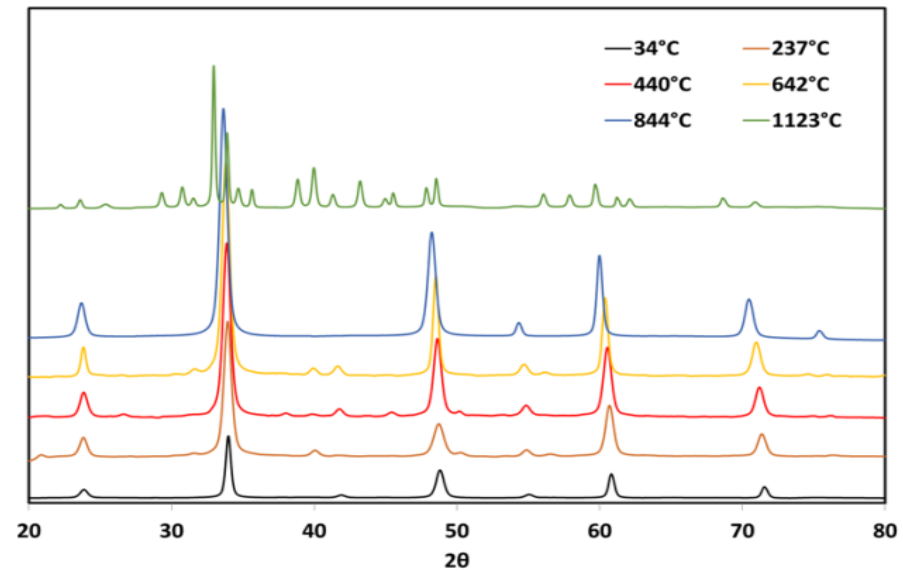
- After 1100°C spinel CaMn$_2$O$_4$ and Ruddlesdon-Popper Ca$_2$MnO$_4$ phases form
- *Irreversible phase transition also observed under isothermal cyclic conditions at lower temperatures*

Motivation for Dopant Addition

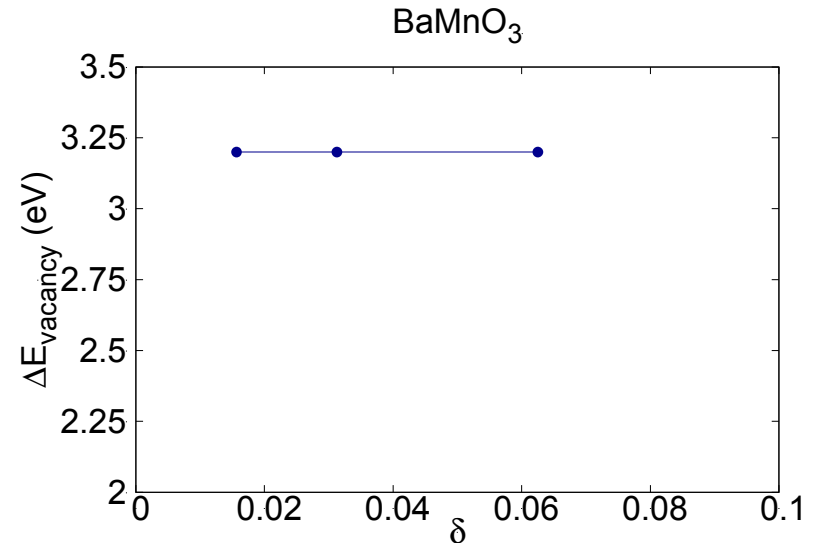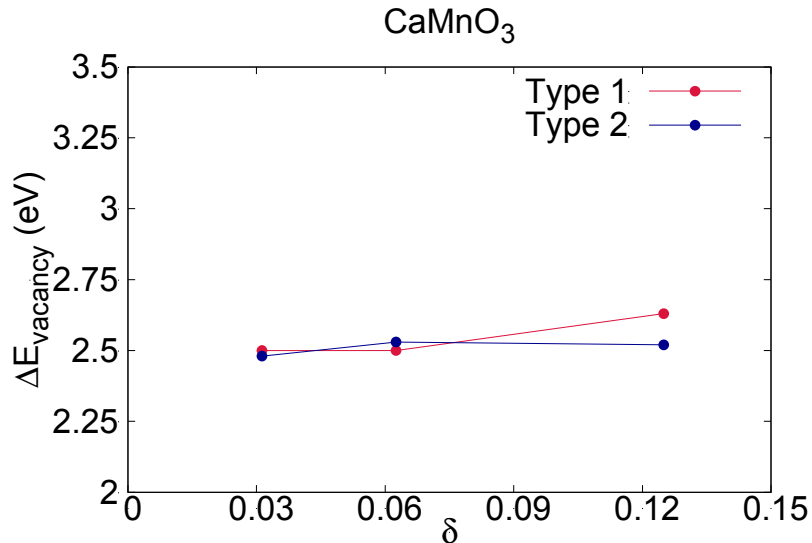| Primary Perovskite Material	CaMnO$_3$
A-site Dopants	Ba and Sr
B-site Dopants	Fe, Co, Ni, V, Al

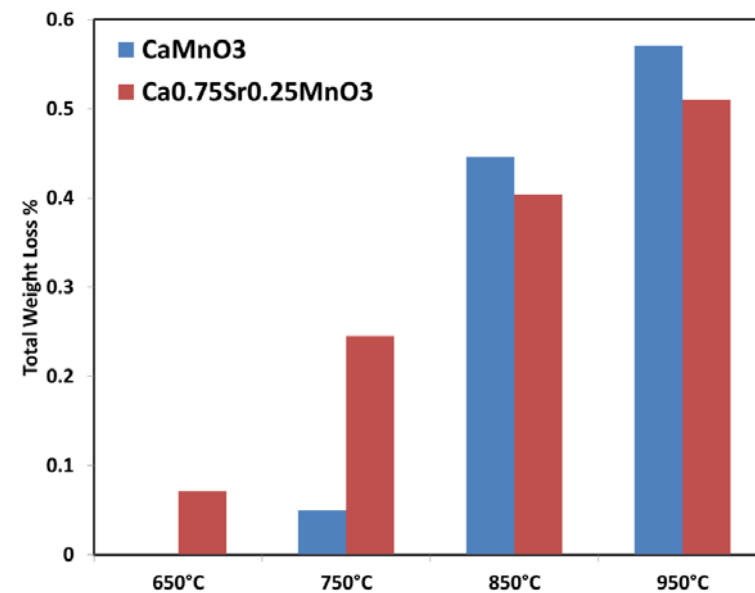**Testing Conditions:**
T: 650-1200°C
P$_{O2}$: <<0.01-0.10atm

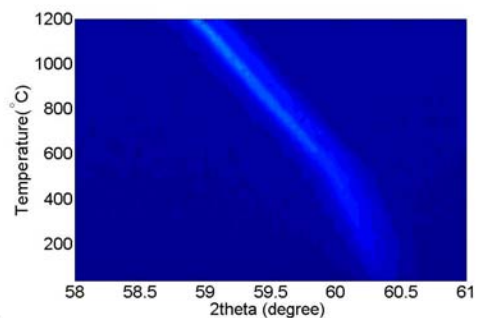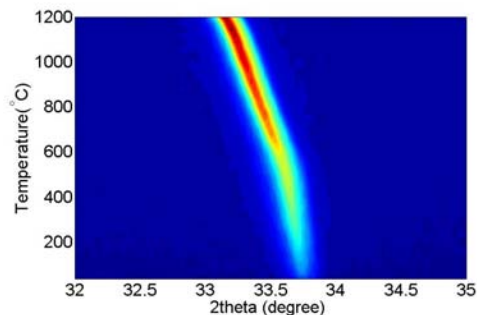**Experiments:**
1) (*In-situ*) XRD
2) Temperature programmed desorption (TPD)
3) Isothermal (chemical looping) cycling
4) Redox cycles with solid fuel

CaMnO$_3$

BaMnO$_3$

Effect of Sr Substitution for CaMnO$_3$

Ca$_{0.75}$Sr$_{0.25}$MnO$_3$
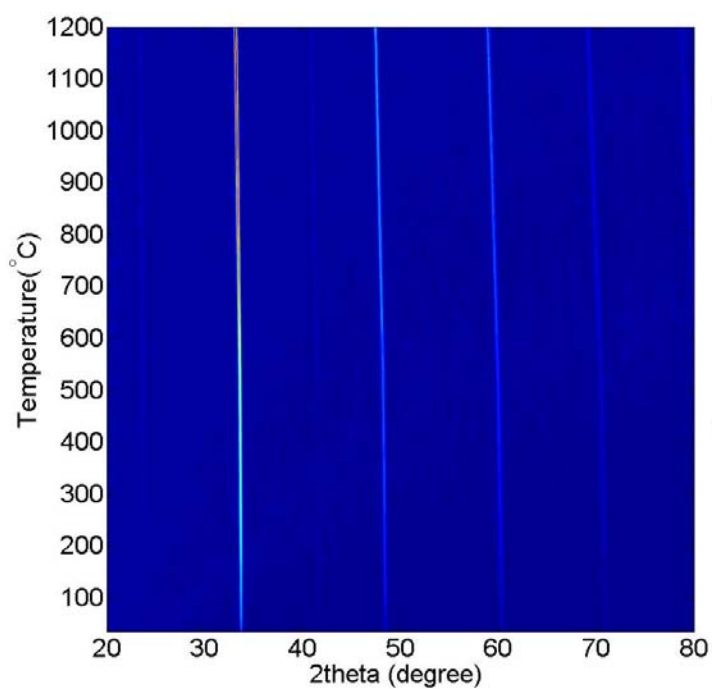
No irreversible phase transition observed; significantly lowered uncoupling temperature

Effect of B-site Substitution for $CaMnO_3$
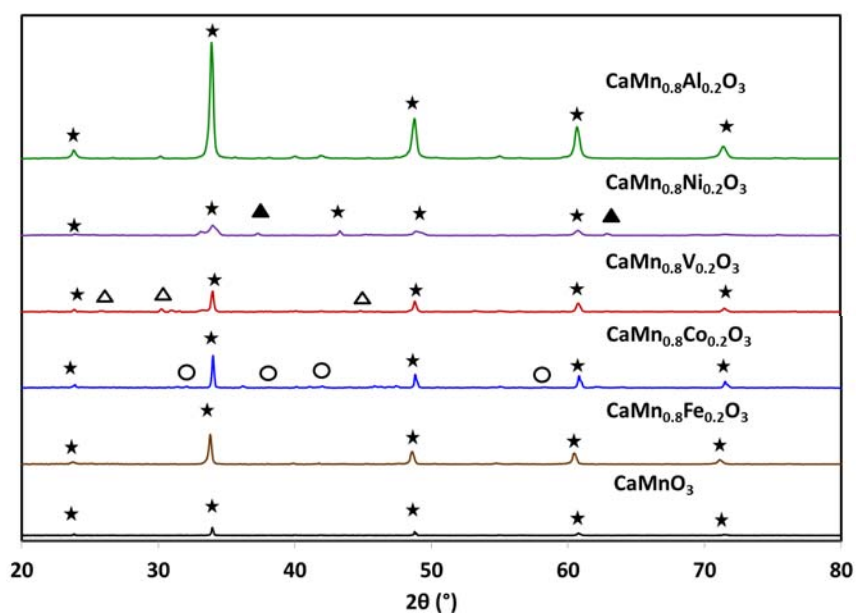
($\star$)$CaMnO_3$ ($\circ$) $Ca_3Co_{1.5}Mn_{0.5}O_6$ ($\triangle$) V_2O_5 and ($\blacktriangle$) NiO phases
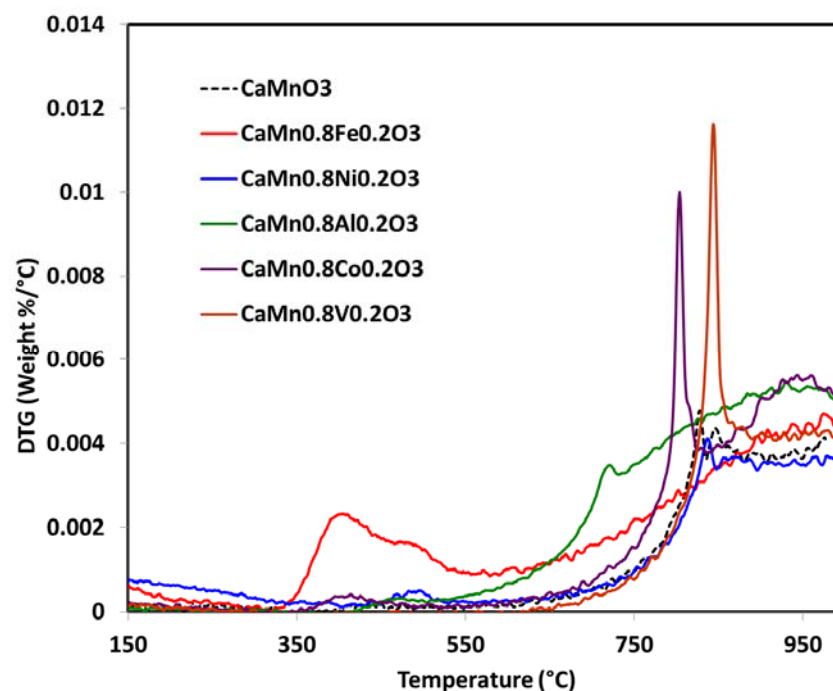
B-site substitution also leads to oxygen carriers with varying oxygen release properties

Effect of B-site Substitution for $CaMnO_3$- Iron
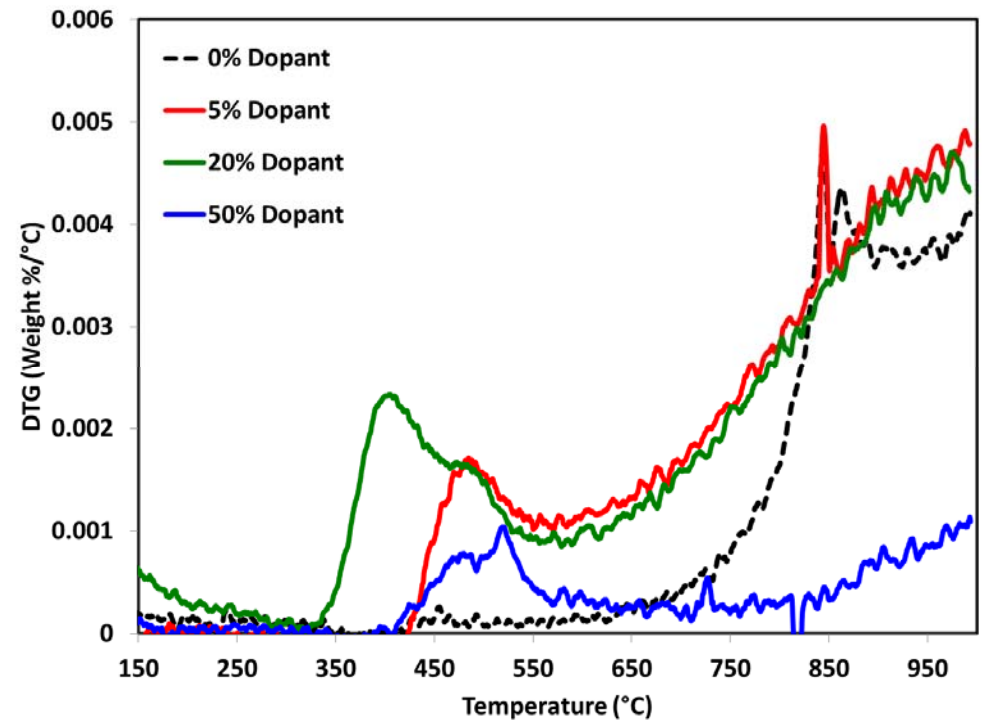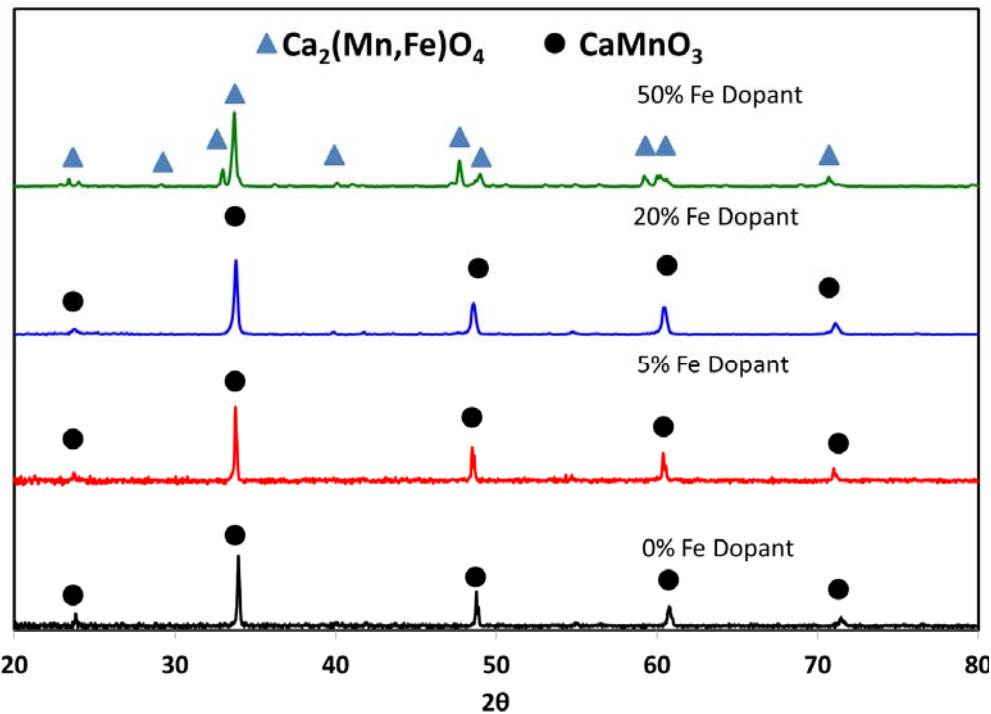
Dopant	a (Å)	b (Å)	c (Å)	Volume (Å³)
N.A.	5.29	7.47	5.27	208.15
5% Fe	5.32	7.41	5.02	197.93

Substitution of Fe into the B-site
- *Formation of solid solution at low Fe concentrations*
- *High Fe concentration induces a Ruddlesden-Popper phase*
- α-oxygen release at low temperatures

Effect of B-site Substitution for $CaMnO_3$- Iron

$CaMn_{0.95}Fe_{0.05}O_3$
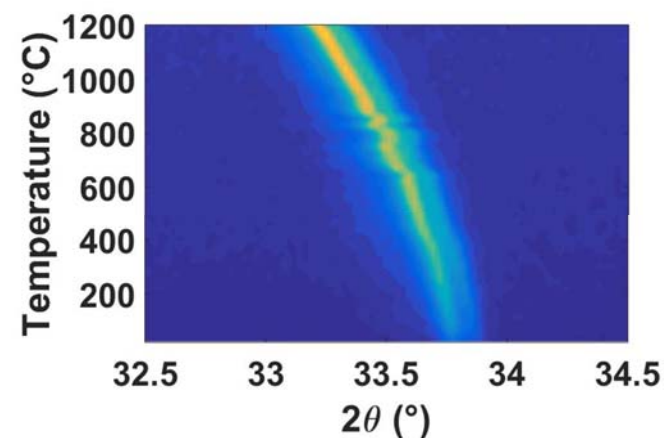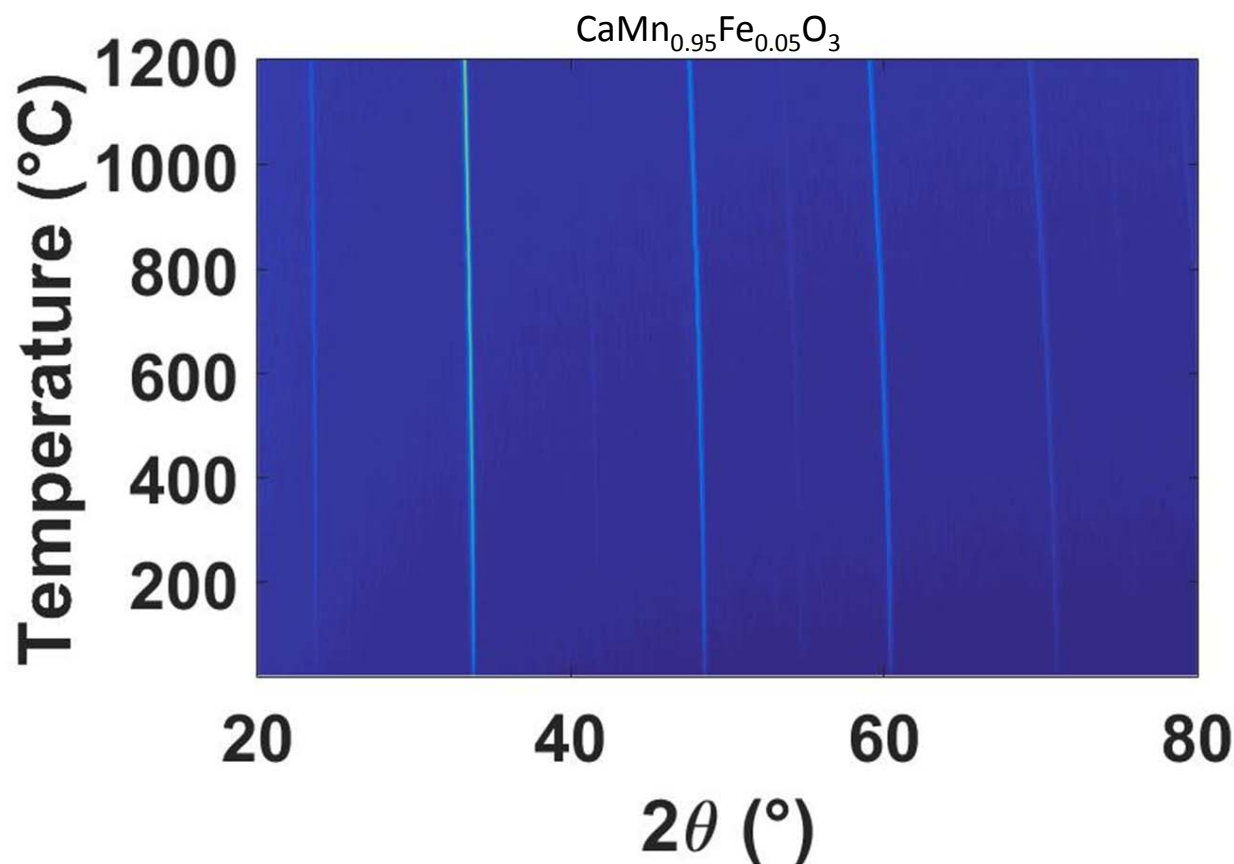
No irreversible phase transition observed up to 1200 ˚C

CLOU Property Comparisons
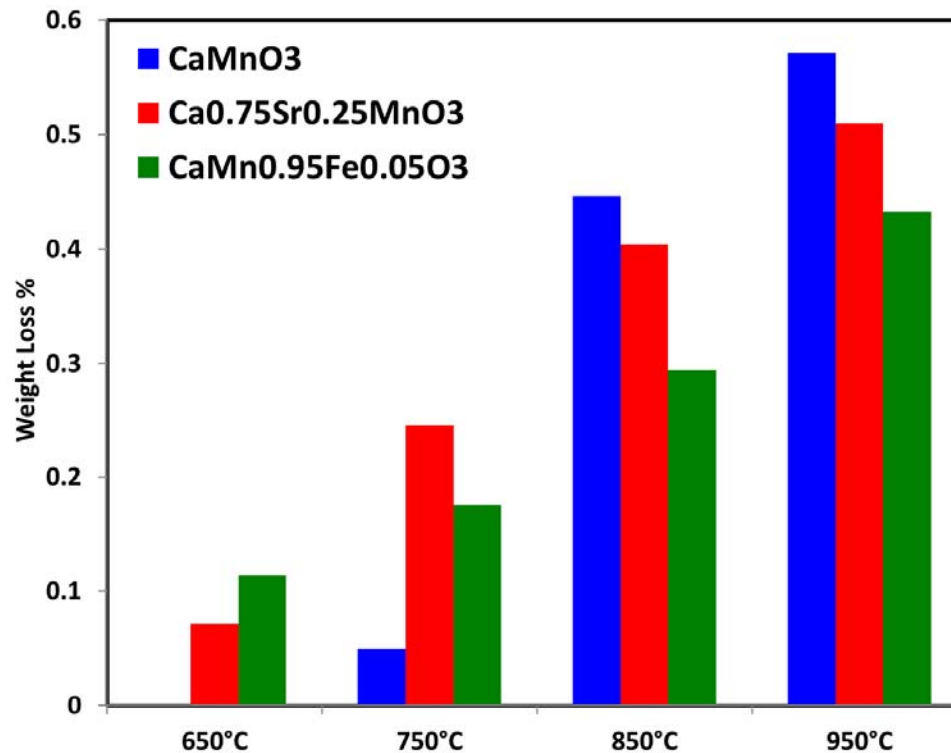
Doping of the A- and B-site of $CaMnO_3$ allows for more low temperature oxygen desorption. $CaMnO_3$ does not observe much oxygen release below 800°C

Isothermal Cycles- Long Term Cycling

$Ca_{0.75}Sr_{0.25}MnO_3$

$CaMn_{0.95}Fe_{0.05}O_3$
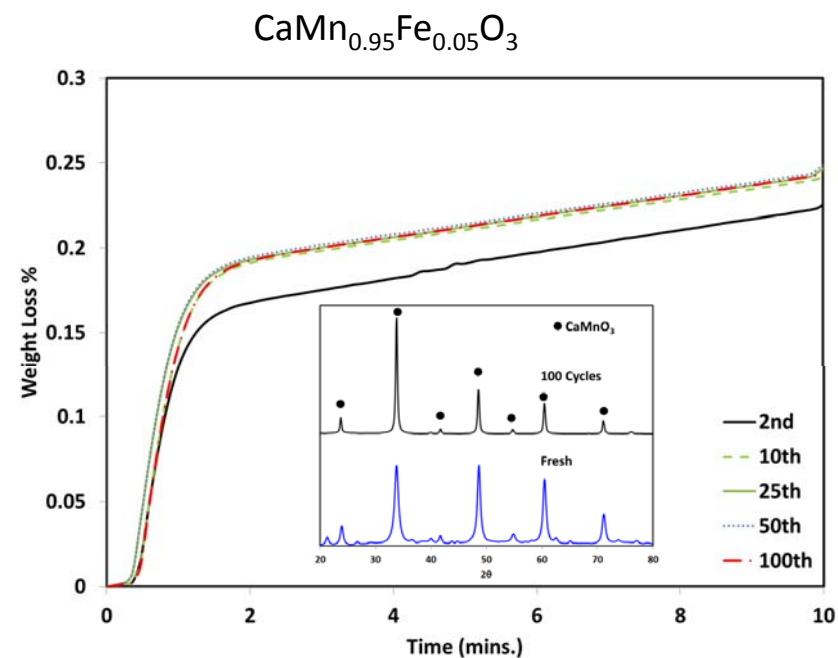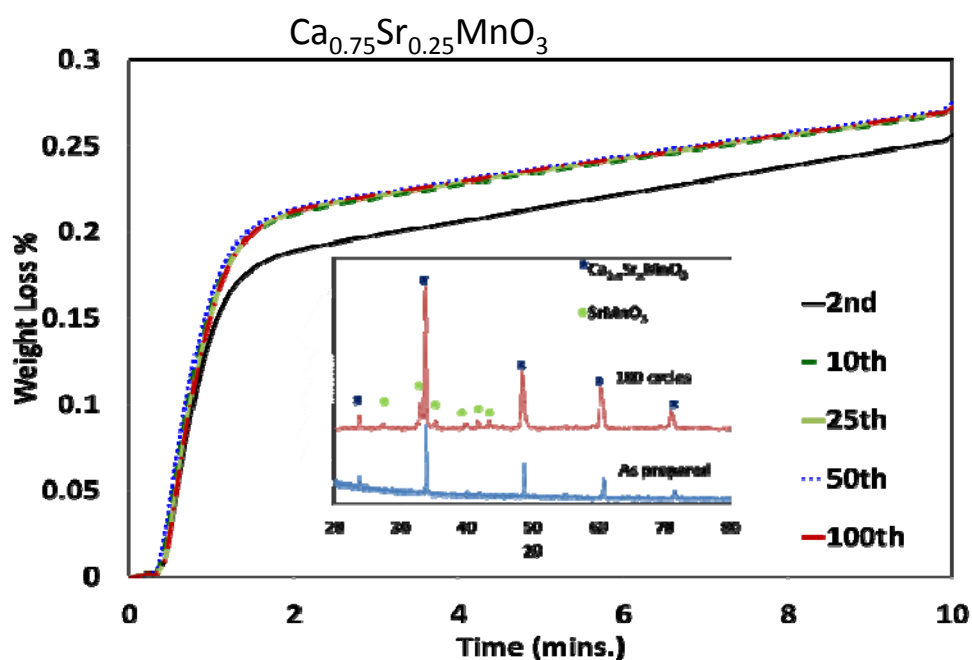
Substituted oxygen carriers are both redox stable for 100+ cycles. No undesirable phase transitions are observed after cycling.

Fluidized Bed Setup
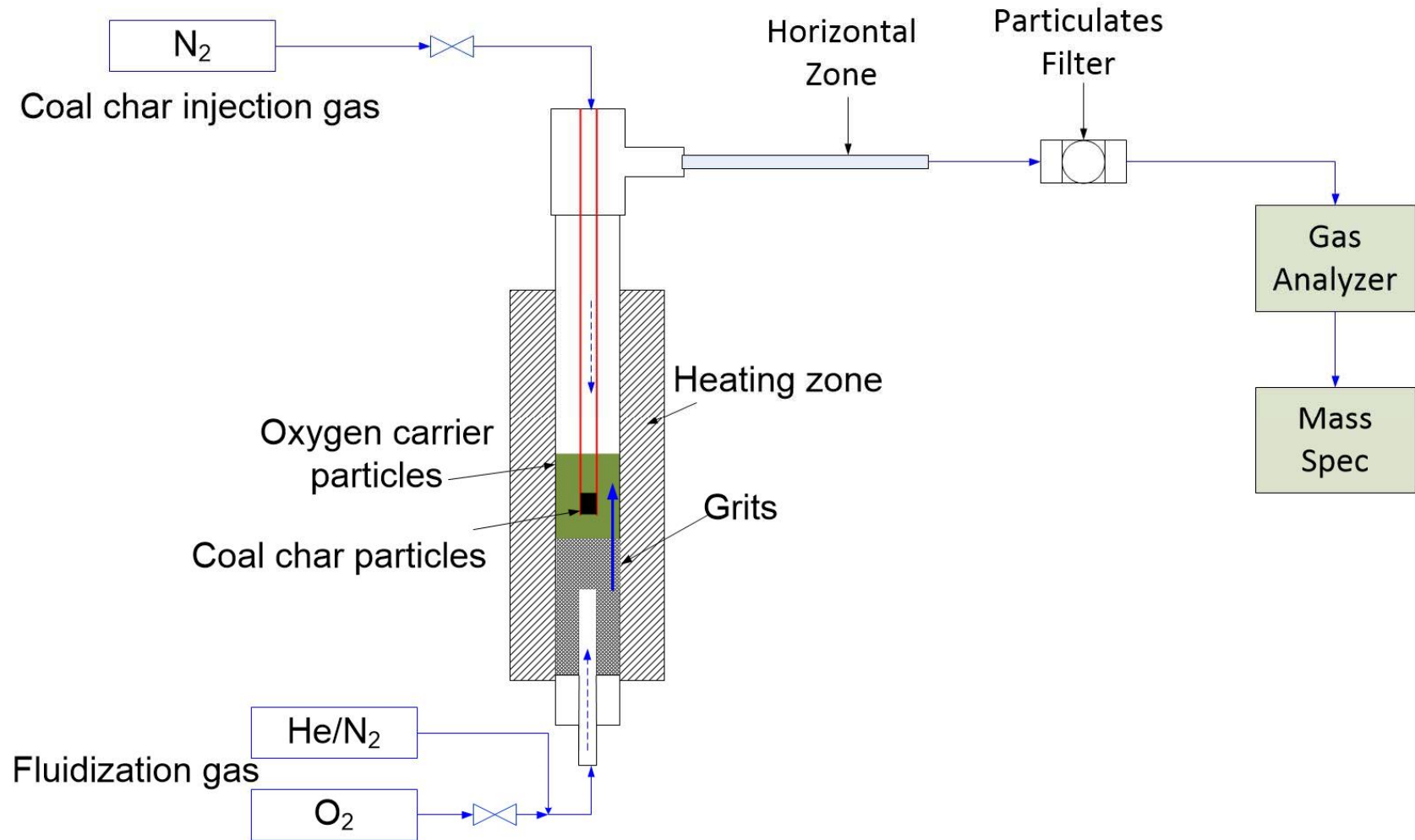
Fluidized Bed Experiments
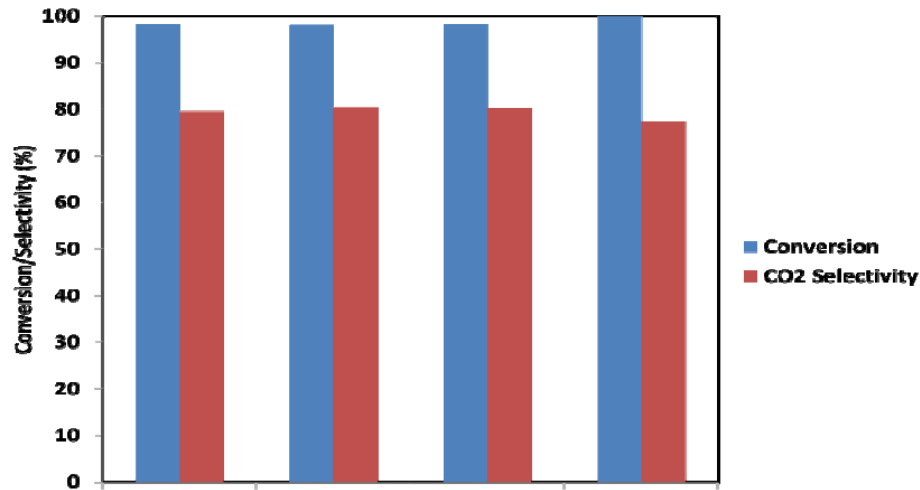
Char cycles after 20 hours operation in helium/10% O_2 redox mode (~60 cycles) and 10 other char cycles spread throughout the 20 hours of operation

Temperature: 850°C
Fluidization velocity: 6 times of U_{mf}
Coal Used: Sea coal (bituminous)
Attrition rate: <0.02%/hour
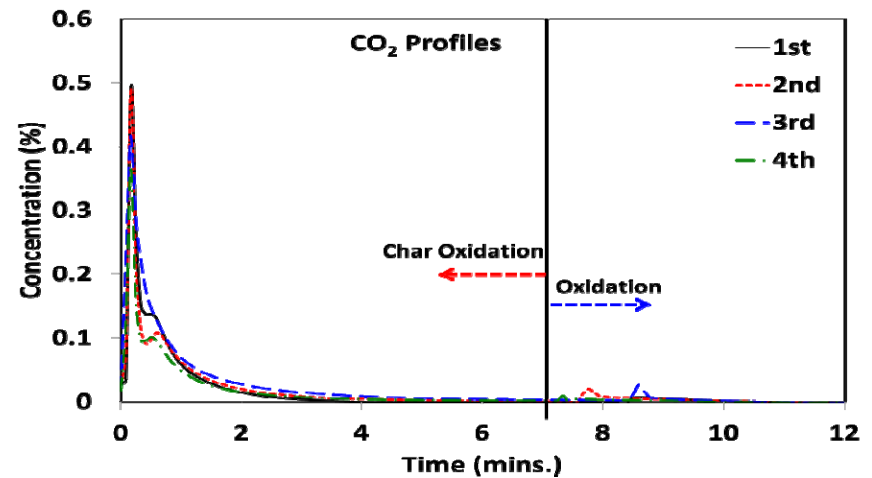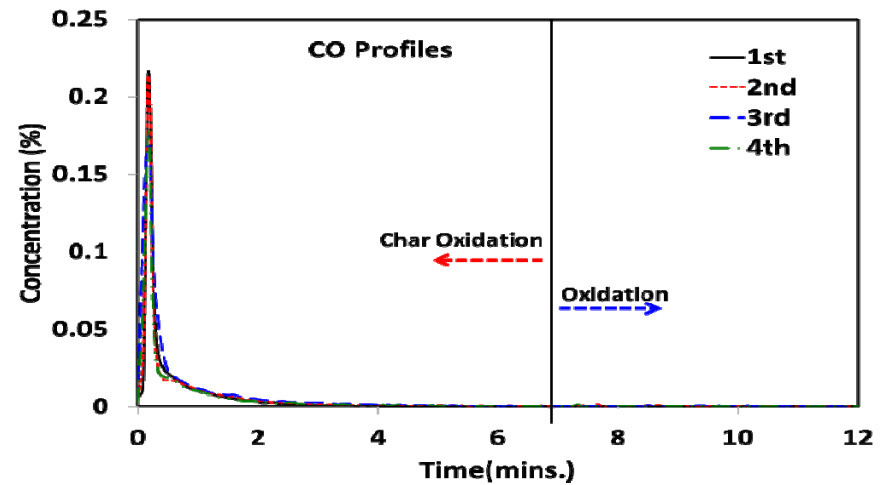
Fluidized Bed-Experiments

$CaMn_{0.95}Fe_{0.05}O_3$-850°C
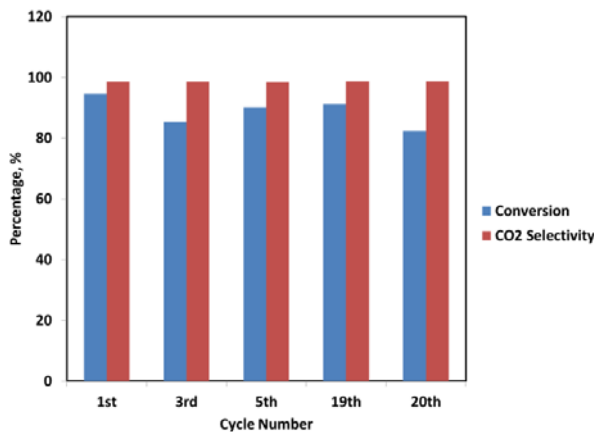
$CaMnO_3$-950°C
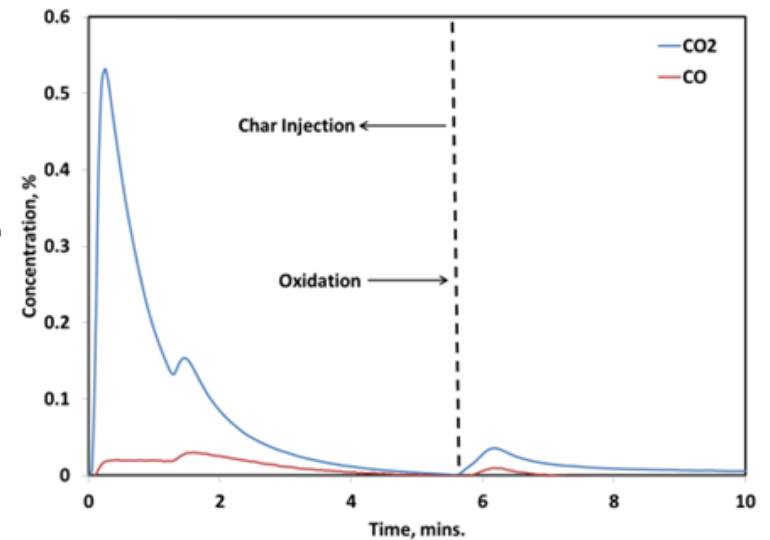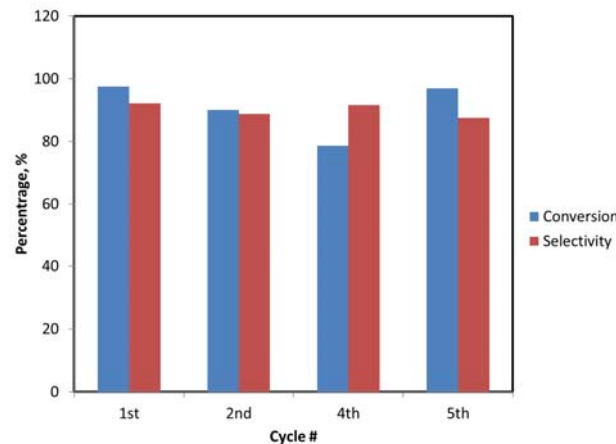
Fluidization velocity: 6 times of U_{mf}
Coal Used: Pittsburgh #8 coal (bituminous)
Attrition rate: <0.01 w.t.%/hour

Undoped $CaMnO_3$ was unable to achieve above 20% conversion at 850°C. Doped perovskites offer better low temperature conversion of coal char particles.

Outline

- Background

- Experimental investigation of $Ca_xA_{1-x}Mn_yB_{1-y}O_3$ based oxygen carriers

- Computational investigation of $Ca_xA_{1-x}Mn_yB_{1-y}O_3$ based oxygen carriers

- Selection criteria for commercially viable oxygen carriers

- Conclusions

Proposed Approach

- Vacancy formation energy can provide thermodynamic basis for estimating CLOU capabilities

- DFT can provide such information via first principle calculations

  Question: how to perform accurate yet efficient calculations?

$$\Delta E_{vacancy} = E_{defect} - E_{perfect} + \frac{1}{2}O_2$$
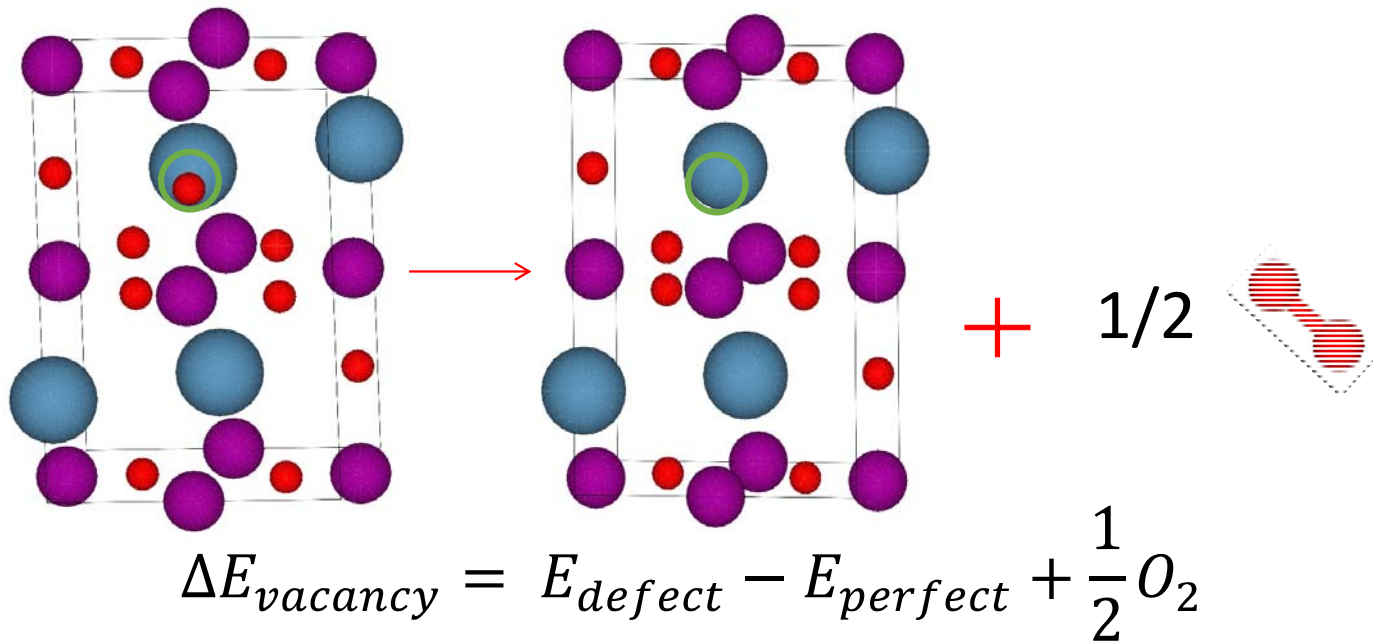
Simulation Strategy

- Practical considerations for efficient DFT screening:
  - Validity of DFT without U
  - Magnetic state considerations
  - Validity of neutral vacancy assumption
  - Vacancy formation energy at dilute limit

- Determination of screening methods:
  - DFT *v.s.* DFT+U
  - Formation energies for different charge states
  - $CaMnO_3$ and $BaMnO_3$ as model compounds

$$\Delta E_{vacancy} = E^q_{defect} - E_{perfect} + \frac{1}{2}O_2 + q(E_F + E_{VBM})$$

Stability of Various Magnetic States
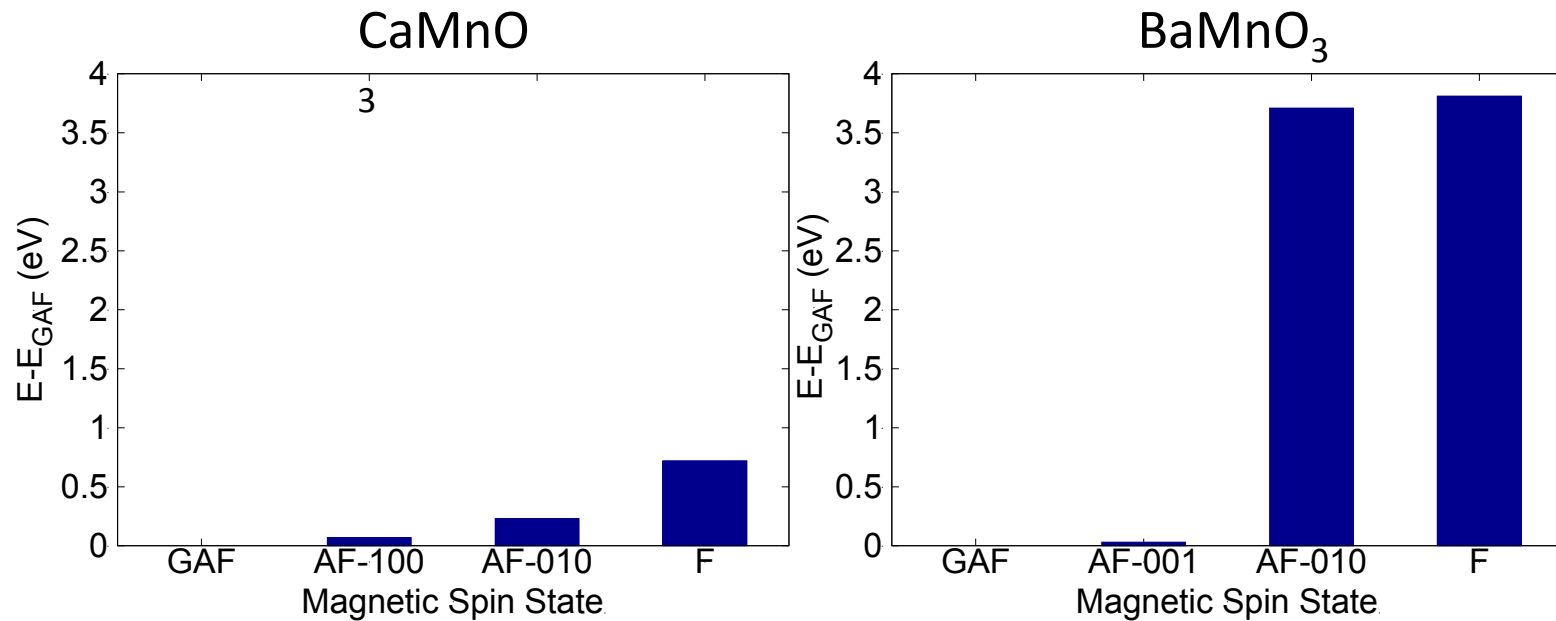
CaMnO

BaMnO$_3$

G-type antiferromagnetic magnetic configuration is found to be the most stable

Vacancy Formation – Dilute Limit without U
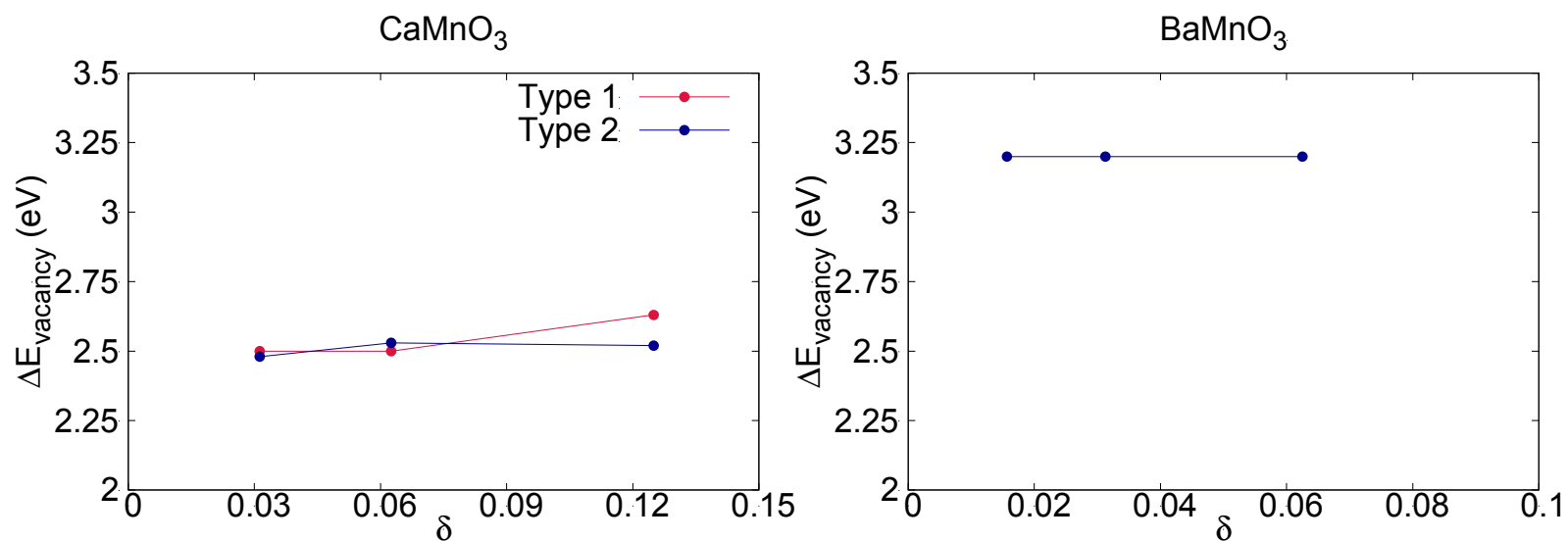
Dilute limit for vacancy formation is observed in both CaMnO₃ and BaMnO₃

Vacancy formation is easier in CaMnO₃ (2.5 eV vs. 3.2 eV)

DFT Validation with DFT + U

CaMnO$_3$ BaMnO$_3$
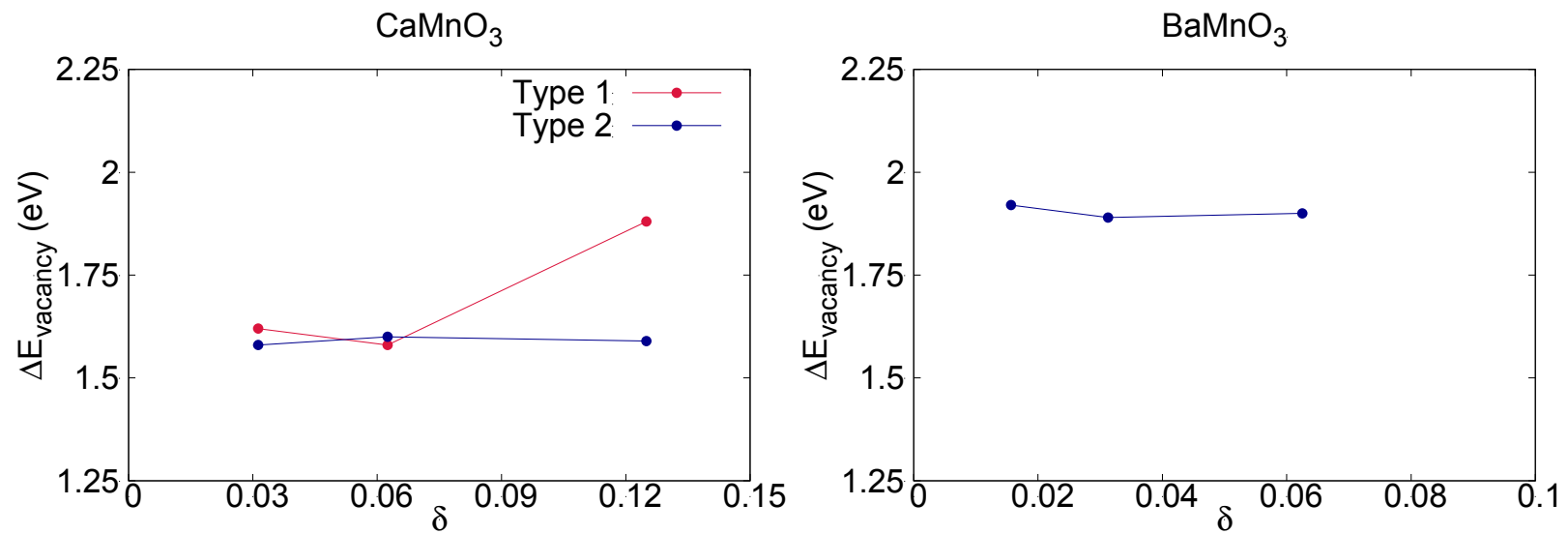
DFT + U does not change the ranking of the materials in terms of ΔE_V

Validation of Neutral Vacancy Assumption

$$\Delta E_{vac.}(q) = E_{defect}^q - E_{perfect} + \frac{1}{2}O_2 + q(E_F + \color{red}{E_{VBM}})$$

$$\Delta E_H(q) = \frac{E_H - E_H(q)}{q}; \lim_{\frac{1}{q} \to \infty} \Delta E_H(q) = E_{VBM}$$
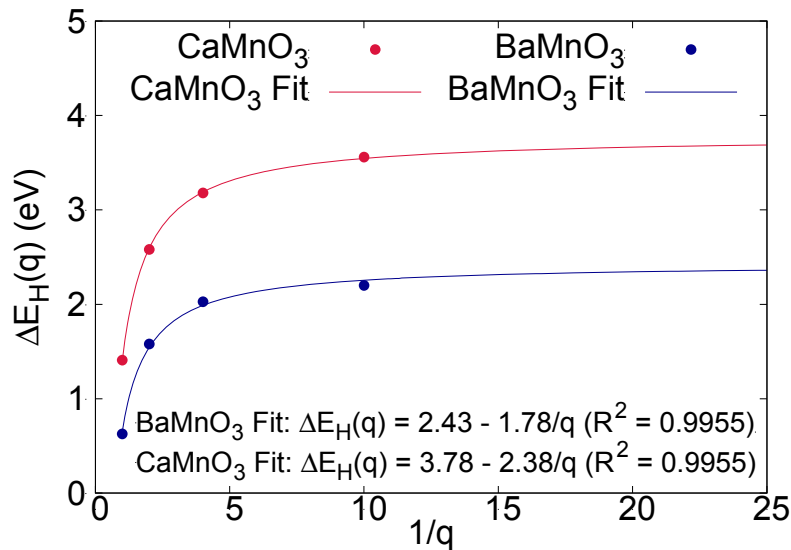
- Valence band maximum needs to be determined
- Energy of dilute hole gas corresponds to this
- $CaMnO_3$: 3.78 eV
- $BaMnO_3$: 2.43 eV

Vacancy Charge Analysis

$$\Delta E_{vac.}(q) = E_{defect}^q - E_{perfect} + \frac{1}{2}O_2 + q(E_F + E_{VBM})$$

CaMnO$_3$

BaMnO$_3$
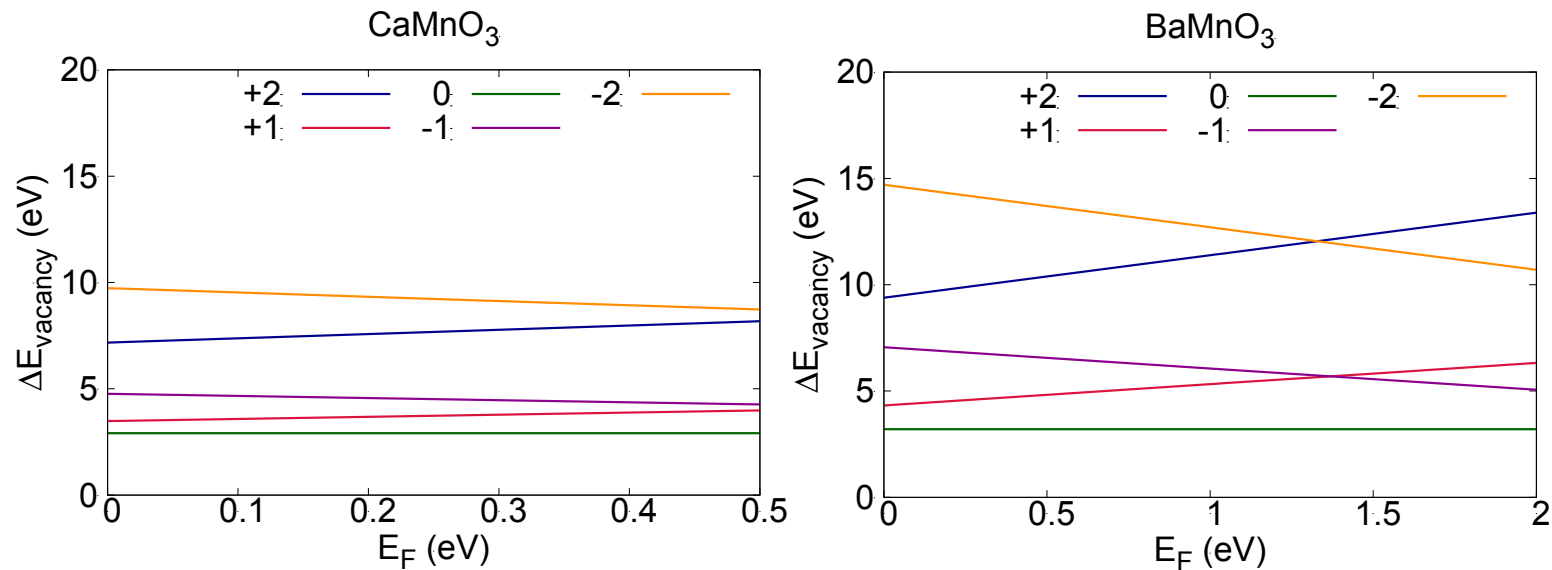
- Each charge state has unique vacancy formation energy across band gap[1,2]

- Neutral vacancy is most stable

1. Ravi, S., Kar, M., Borah, S. M. & Krishna, P. S. R. *Cryst. Res. Technol.* **43,** 1318–1322 (2008).
2. Cussen, E. J. & Battle, P. D. **12,** 831–838 (2000).

Extension to $Ca_{0.75}Sr_{0.25}MnO_3$ and $CaMn_{0.75}Fe_{0.25}O_3$

Substitution
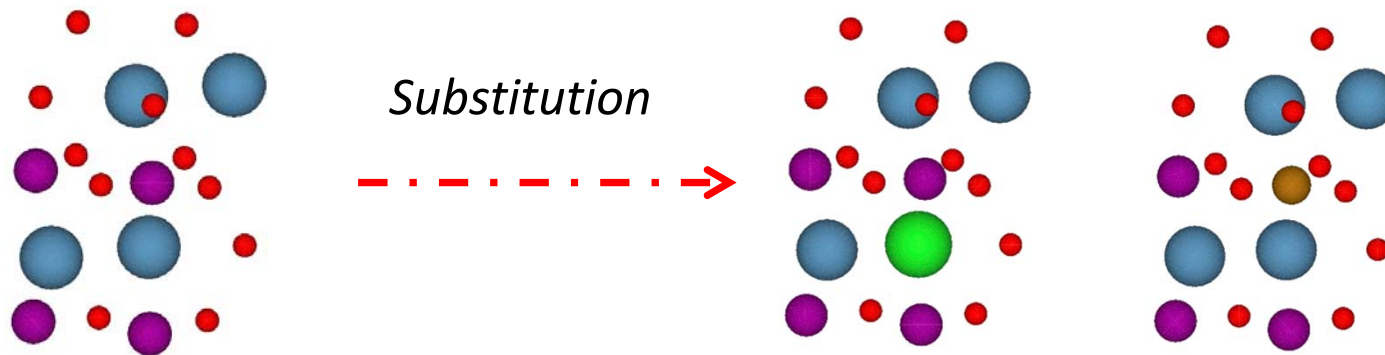
- Generate structures by replacing Ca and Mn in $CaMnO_3$ with Sr an Fe, respectively

- After relaxation, symmetry may be become broken -> requires efficient evaluation oxygen types in the structures

Ca$_{0.75}$Sr$_{0.25}$MnO$_3$: Unique Oxygen Types

Oxygen Type	1 (Å)	2 (Å)	3 (Å)	4 (Å)	5 (Å)
1a	Mn (1.93)	Mn (1.93)	Ca (2.34)	Sr (2.43)	
1b	Mn (1.92)	Mn (1.92)	Ca (2.42)	Sr (2.43)	
2a	Mn (1.89)	Fe (1.89)	Ca (2.33)	Ca (2.48)	
2b	Mn (1.90)	Mn (1.90)	Ca (2.34)	Ca (2.43)	
3a	Mn (1.91)	Mn (1.92)	Ca (2.35)	Ca (2.60)	Sr (2.63)
3b	Mn (1.91)	Mn (1.92)	Ca (2.37)	Ca (2.57)	Sr (2.65)
4	Mn (1.92)	Mn (1.92)	Ca (2.36)	Ca (2.52)	Ca (2.66)
5	Mn (1.90)	Mn (1.90)	Sr (2.44)	Ca (2.58)	Ca (2.59)
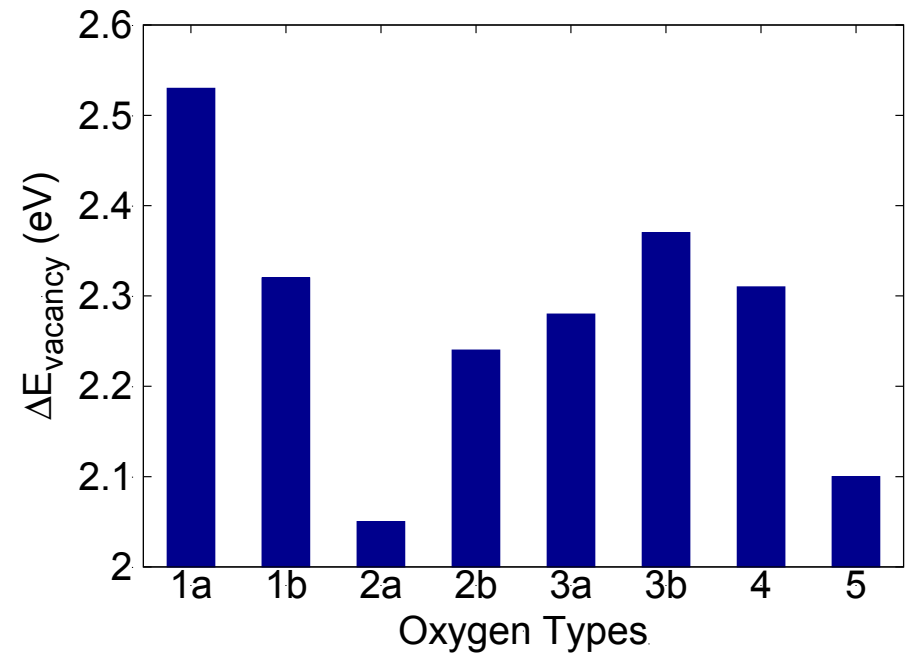
Evaluation of local environment reveals type 2a and 5 correspond to easiest vacancy formation

$Ca_{0.75}Sr_{0.25}MnO_3$ Dilute Limit
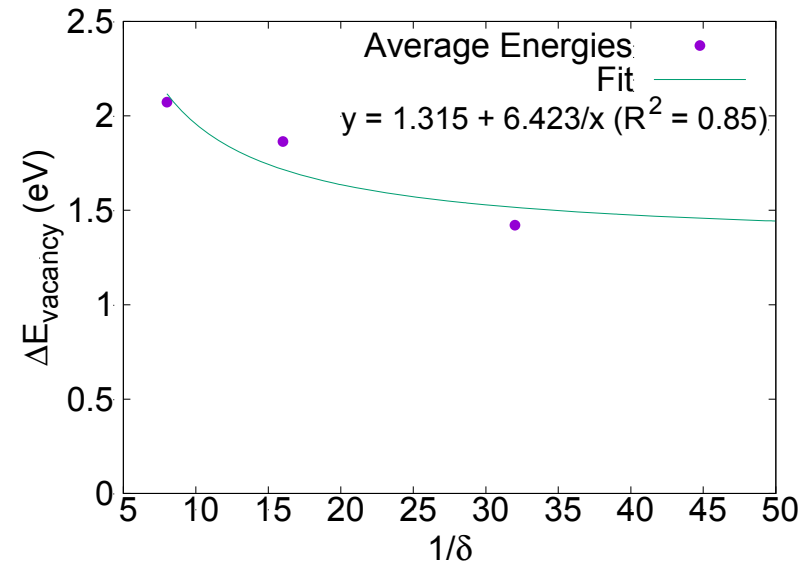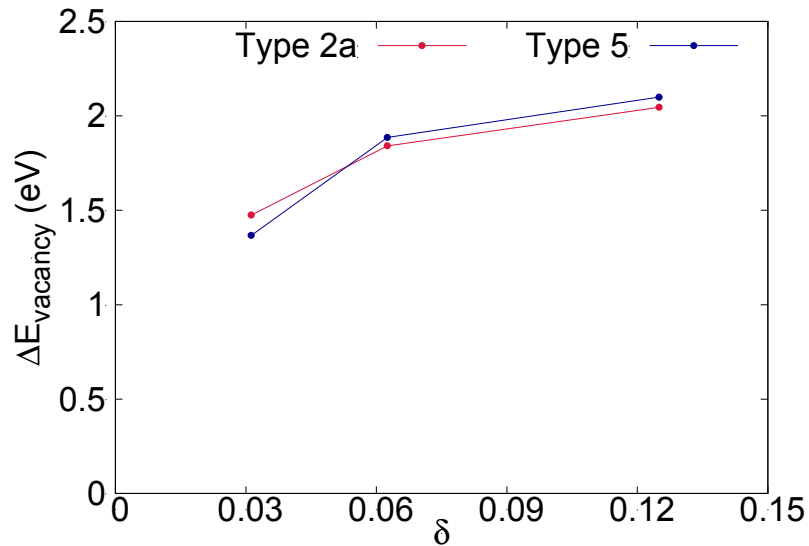
- Type 2a and Type 5 appear indistinguishable
- Curve fitting reveals dilute limit: 1.315 eV

CaMn$_{0.75}$Fe$_{0.25}$O$_3$: Unique Oxygen Types

Oxygen Type	1 (Å)	2 (Å)	3 (Å)	4 (Å)	5 (Å)
1	Mn (1.91)	Fe (1.92)	Ca (2.33)	Ca (2.57)	Ca (2.59)
2	Mn (1.91)	Mn (1.91)	Ca (2.32)	Ca (2.40)	
3	Mn (1.89)	Fe (1.92)	Ca (2.32)	Ca (2.42)	
4	Mn (1.91)	Mn (1.92)	Ca (2.33)	Ca (2.54)	Ca (2.59)

Evaluation of neighboring cations reveals type 1 and type 3 are easier to remove

CaMn$_{0.75}$Fe$_{0.25}$MnO$_3$ Dilute Limit
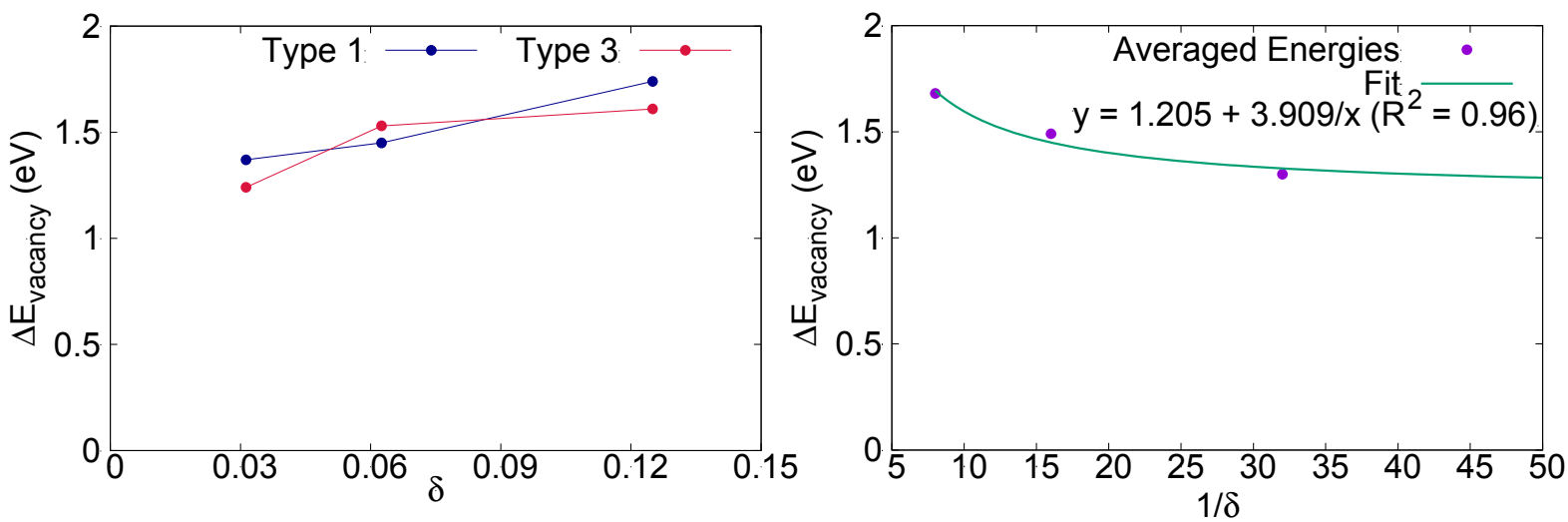
- Type 1 and Type 3 appear indistinguishable
- Curve fitting reveals dilute limit of 1.205 eV

Oxygen Carrier Comparisons
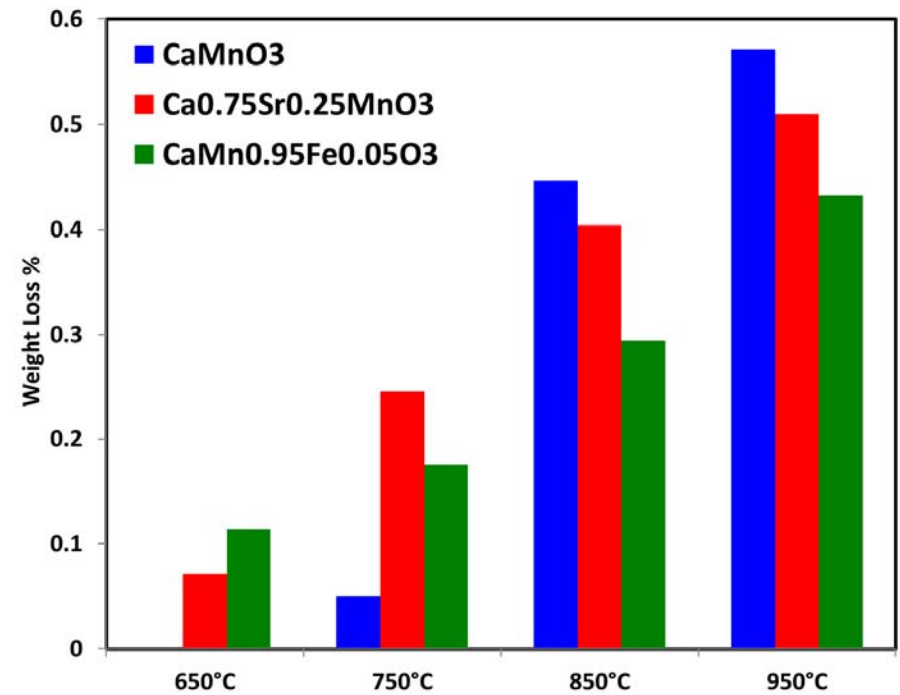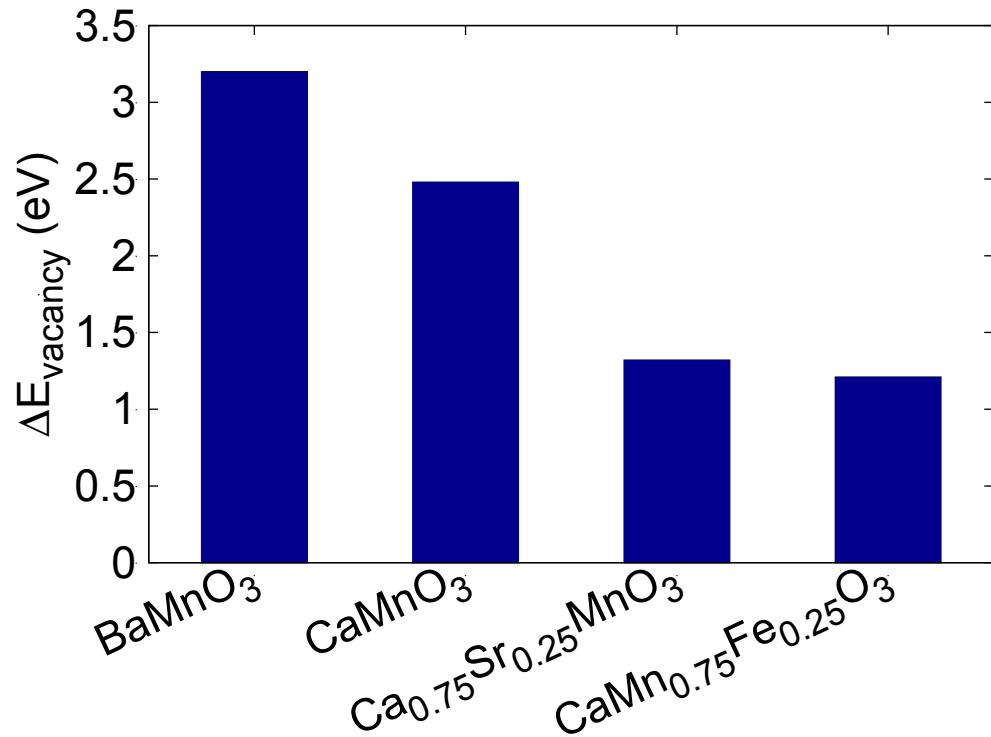
Vacancy formation energy correlate well with oxygen uncoupling temperature

ReaxFF force field parameterization

Use existing and in development ReaxFF parameters for most interactions
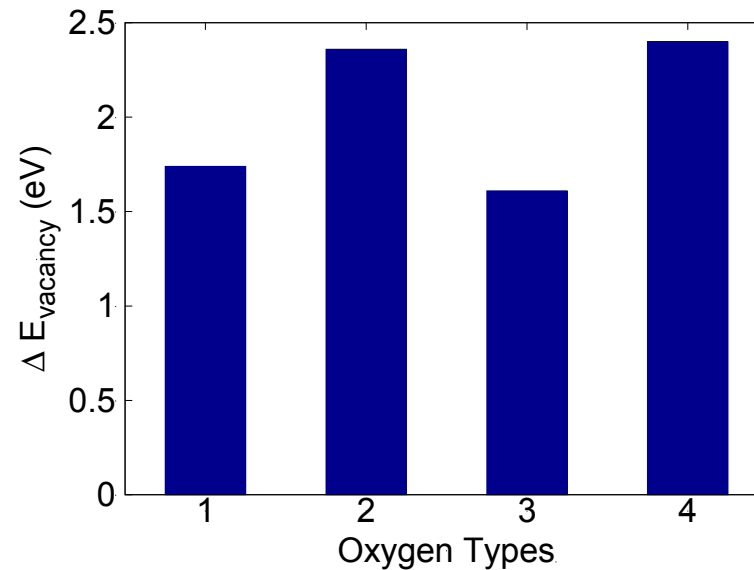
Existing metal ReaxFF force fields
for metal oxides[1,2]
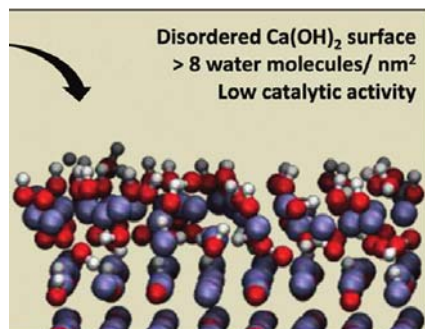
In development MnO[3] ReaxFF force field

Disordered Ca(OH)$_2$ surface
> 8 water molecules/ nm^2
Low catalytic activity
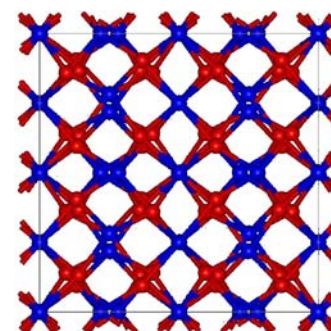
Parameterize missing metal-Mn interactions using DFT derived crystal and defect energies

1. CaO: H. Manzano … A. C. T. van Duin. Langmuir 28 4187-4197 **2012**.
2. BaO: A. C. T. van Duin … W. A. Goddard III. Phys. Chem. A. 112 11414-11422 **2008**.

3. A. C. T. van Duin and coworkers. In progress.

Outline

- Background

- Experimental investigation of $Ca_xA_{1-x}Mn_yB_{1-y}O_3$ based oxygen carriers

- Computational investigation of $Ca_xA_{1-x}Mn_yB_{1-y}O_3$ based oxygen carriers

- Selection criteria for commercially viable oxygen carriers

- Conclusions

Reactor Scale Up Considerations

Parameter	Literature	Scale-Up
Power	1.5 kW_{th}	1000 MW_{th}
Oxygen Carrier	CuO	$CaMnO_3$
Solids Inventory (kg/MW_{th})	100-250	350
Solids Fraction	0.45	0.45
Density (kg/L)	4.6	2.5
Reactor Volume Inventory (L/MW_{th})	40-120	310
Reactor Dimensions	50mm x 200mm	7.3m x 7.3m
Linear Velocity (m/s) in the inlet	0.11	0.11
Linear Velocity (m/s) at the outlet Assuming 100% conversion of coal	0.5	9
Coal Heating Value (MJ/kg)	20-35	25.9
Coal Feed Rate (tonne/hr)	0.00011	139.1
Solids Circulation Rate (tonne/hr)	0.0042	35,000

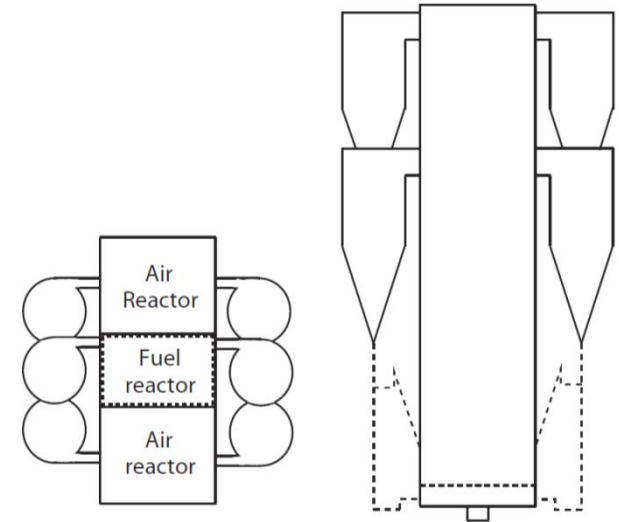1. Abad, A. et al. Demonstration of chemical-looping with oxygen uncoupling (CLOU) process in a 1.5kWth continuously operating unit using a Cu-based oxygen-carrier. Int. J. Greenh. Gas Control **6,** 189–200 (2012).

2. García-Labiano, F., de Diego, L. F., Adánez, J., Abad, A. & Gayán, P. Reduction and Oxidation Kinetics of a Copper-Based Oxygen Carrier Prepared by Impregnation for Chemical-Looping Combustion. Ind. Eng. Chem. Res. **43,** 8168–8177 (2004).

3. Eyring, E. M. et al. Chemical Looping with Copper Oxide as Carrier and Coal as Fuel. Oil Gas Sci. Technol. – Rev. D'IFP Energ. Nouv. **66,** 209–221 (2011).

4. Markström, P., Linderholm, C. & Lyngfelt, A. Chemical-looping combustion of solid fuels – Design and operation of a 100kW unit with bituminous coal. Int. J. Greenh. Gas Control **15,** 150–162 (2013).

5. Berguerand, N. & Lyngfelt, A. Design and operation of a 10kWth chemical-looping combustor for solid fuels – Testing with South African coal. Fuel **87,** 2713–2726 (2008).

6. Sahir, A. H., Sohn, H. Y., Leion, H. & Lighty, J. S. Rate Analysis of Chemical-Looping with Oxygen Uncoupling (CLOU) for Solid Fuels. Energy Fuels **26,** 4395–4404 (2012).

7. Anders Lyngfelt and Bo Leckner. A 1000 MWth boiler for chemical-looping combustion of solid fuels – discussion of design and costs. Applied Energy **157,** 475-487 (2015)

Kinetics- Gas vs Solids
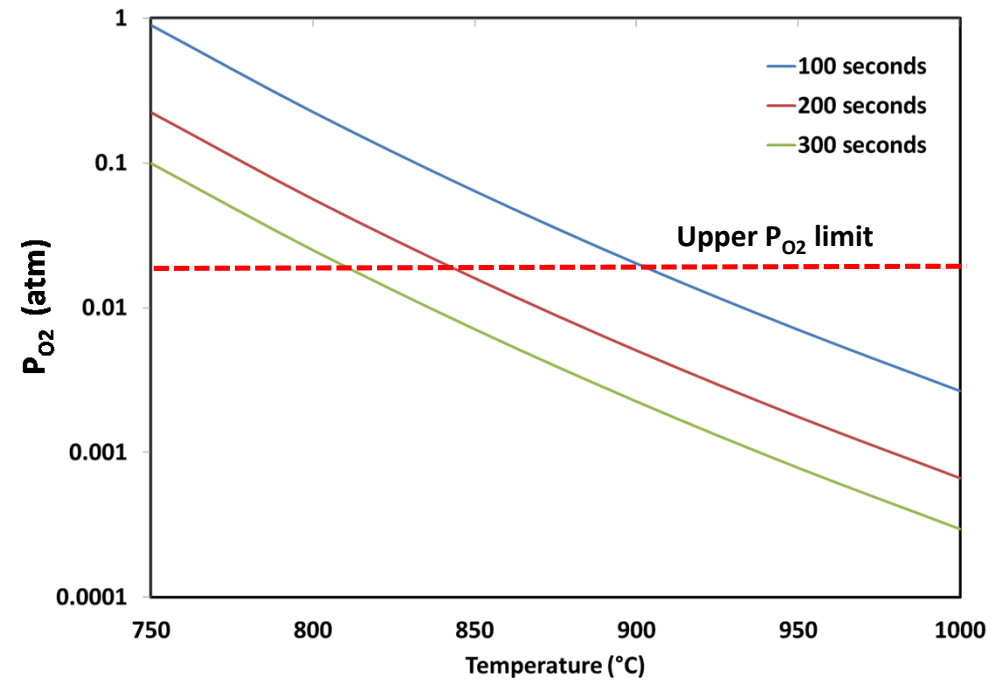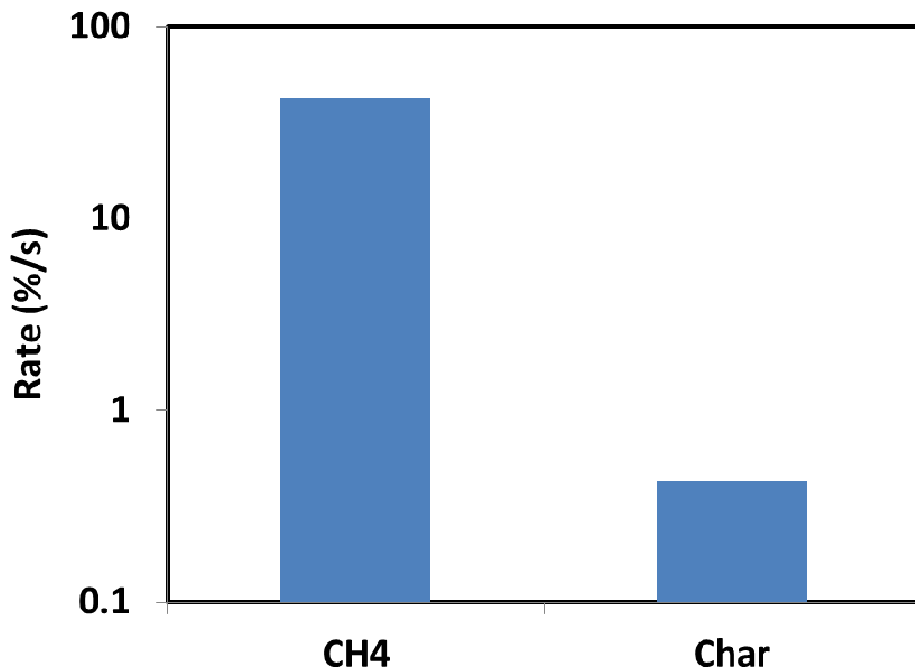
Over two order of magnitude faster kinetics for CH$_4$ when compared to bituminous char. A "critical" P$_{O2}$ range can be determined by char combustion kinetics.

Determination of Critical P_{O2} Range

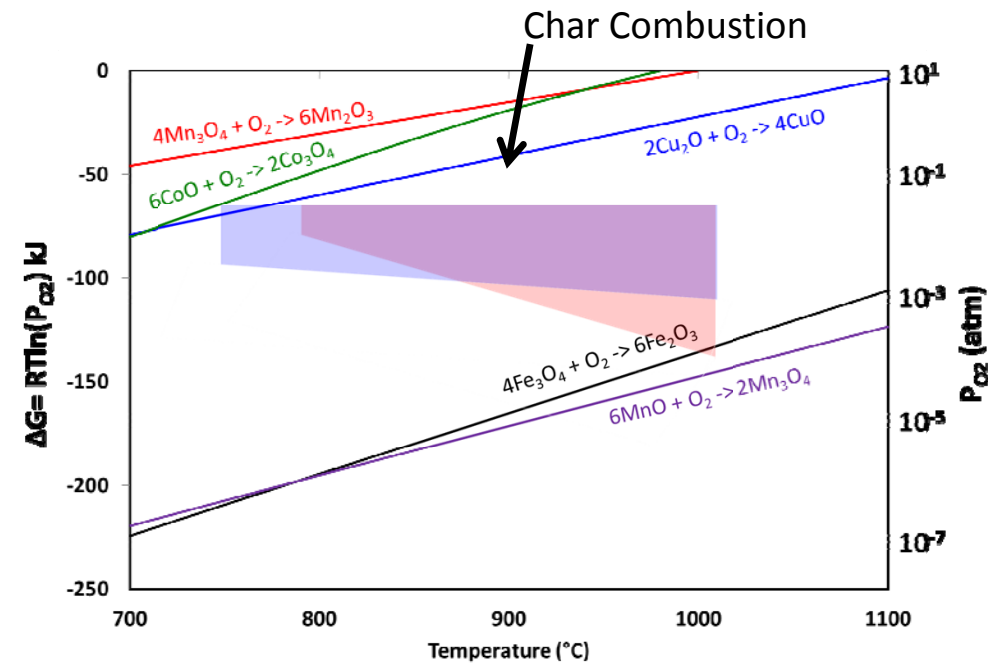| Residence time of coal (s)		200
Parameters:	Experimental	Literature
Model	Arrhenius	Shrinking Core
Coal Type:	Illinois #6 (bituminous)	Pocahontas (bituminous)
Order of reaction (n)	0.92	0.5-1 (0.5 used)
Activation Energy (kJ/mol)	28	126
Pre-exponential factor (A)	414.3 atm$^{-0.92}$s^{-1}	930 g•cm^{-2}atm$^{-0.5}$s^{-1}
Temperature (°C)	950	950
Equilibrium P_{O2} (atm)	0.013	0.0032

Char Combustion

$4Mn_3O_4 + O_2 \rightarrow 6Mn_2O_3$
$6CoO + O_2 \rightarrow 2Co_3O_4$
$2Cu_2O + O_2 \rightarrow 4CuO$
$4Fe_3O_4 + O_2 \rightarrow 6Fe_2O_3$
$6MnO + O_2 \rightarrow 2Mn_3O_4$

$\Delta G = RTln(P_{O2})$ kJ

P_{O2} (atm)

Temperature (°C)

1. Sahir, A. H., Sohn, H. Y., Leion, H. & Lighty, J. S. Rate Analysis of Chemical-Looping with Oxygen Uncoupling (CLOU) for Solid Fuels. *Energy Fuels* **26,** 4395–4404 (2012).

2. Tian, X., Su, M., Zhao, H., Kinetics of lignite char gasification and combustion in rich-CO_2 and/or lean-O_2 atmosphere: A similar condition in coal-derived CLOU processes. Proceedings of the Combustion Institute. (accepted)

Summary

- A-site and B-site substitution in $CaMnO_3$ can enhance its redox stability and oxygen release properties

- DFT with GAF and neutral defect assumptions can correlate with experimental data well and can be used to guide oxygen carrier development

- Char combustion is rate limiting for CLC

- Critical P_{O2} ranges can be determined based on char combustion kinetics and used to guide oxygen carrier optimization

Journal Articles

- Nathan Galinsky and Fanxing Li "CaMn$_{1-x}$B$_x$O$_3$ (B=Al, V, Fe, Co, and Ni) Perovskite Based Oxygen Carriers for Chemical Looping with Oxygen Uncoupling (CLOU)" Applied Energy, 2016 (In-Press)

- Amit Mishra, Nathan Galinsky, Feng He, Erik Santiso, and Fanxing Li "Perovskite-structured AMn$_x$B$_{1-x}$O$_3$ (A= Ca or Ba; B= Fe or Ni) redox catalysts for partial oxidation of methane." Catal. Sci. Technol., 2016 DOI: 10.1039/C5CY02186C

- Nathan Galinsky, Arya Shafiefarhood, Yanguang Chen, Luke Neal, Fanxing Li "Effect of support on redox stability of iron oxide for chemical looping conversion of methane". Applied Catlaysis B: Environmental. 2015, 164: 371-379.

- Nathan Galinsky, Amit Mishra, Jia Zhang, and Fanxing Li* "Ca$_{1-x}$A$_x$MnO$_3$ (A= Sr and Ba) Perovskite Based Oxygen Carriers for Chemical Looping with Oxygen Uncoupling (CLOU)". Applied Energy, 2015 DOI:10.1016/j.apenergy.2015.04.020

- Arya Shafiefarhood, Amy Stewart, Fanxing Li* "Iron-Containing Mixed-Oxide Composites as Oxygen Carriers for Chemical Looping with Oxygen Uncoupling (CLOU)". Fuel. 2015, 139: 1-10

- Mishra A, Santiso E, Li F. "Screening of AMnO$_3$ perovskites for chemical looping with oxygen uncoupling (CLOU) through first principles calculations of oxygen vacancy formation energy." (in preparation)

Conference Presentations

- Arya Shafiefarhood, Nathan Galinsky, and Fanxing Li. "Mixed-oxides for carbonaceous fuel conversion with integrated CO2 capture via chemical looping with oxygen uncoupling (CLOU)" 248th ACS National Meeting. San Francisco, CA. August 2014.

- Arya Shafiefarhood, Nathan Galinsky, Amit Mishra, and Fanxing Li. "Composite mixed oxides for chemical looping with oxygen uncoupling." 3rd International Conference on Chemical Looping. Gothenburg, Sweden. 10 September 2014. Conference Presentation.

- Nathan Galinsky, Amit Mishra, and Fanxing Li. "Perovskite Based Oxygen Carriers for Chemical Looping with Oxygen Uncoupling." 2014 AICHE Annual Meeting. Atlanta, GA. 19 November 2014.

- Mishra A, Santiso E, Li F. Perovskite Structured Redox Catalysts for Methane Partial Oxidation Using Lattice Oxygen. *2015 ACS, Boston, MS*.

Acknowledgement

- Prof. Erik Santiso (Co-PI)
- Graduate Students:
  - Amit Mishra
  - Nathan Galinsky
  - Arya Shafiefarhood
- Undergraduate Students:
  - Lindsay Bowers
  - Grant Thomas
  - Rory Bergen
- Funding:
  - US DOE FE001247
- Project Managers
  - Jason Hissam and David Lyons

Thanks!

Preliminary Results: Climbing Image NEB of $E_{barrier}$ for oxygen vacancy migration

Energy barrier for oxygen vacancy migration is lower for $CaMnO_3$
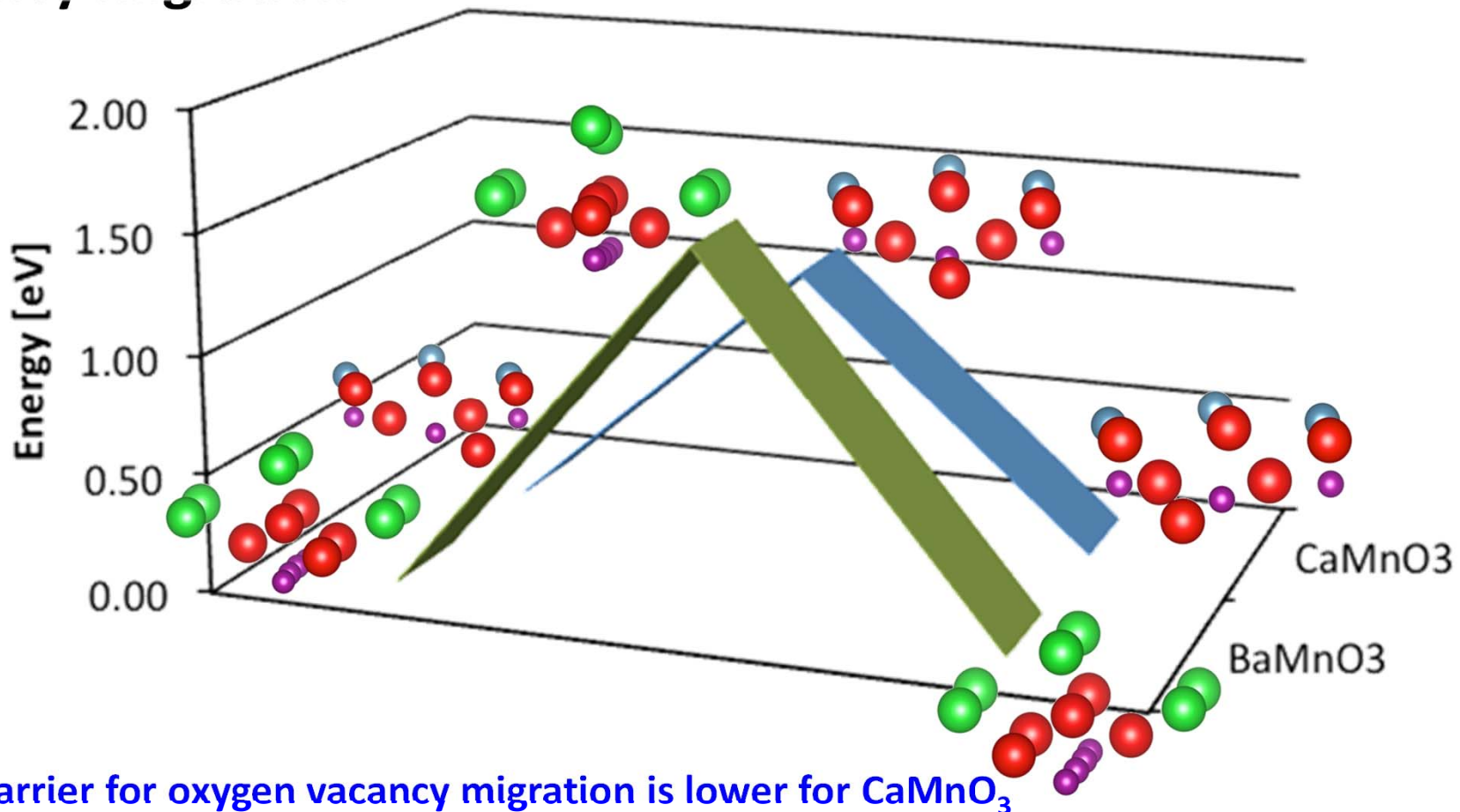
DFT Parameters

VASP package

Electron Ion Interaction: PAW

Exchange correlation functional: PBE-GGA

Energy cut-off: 425 eV

EDIFF = 10^{-4} eV

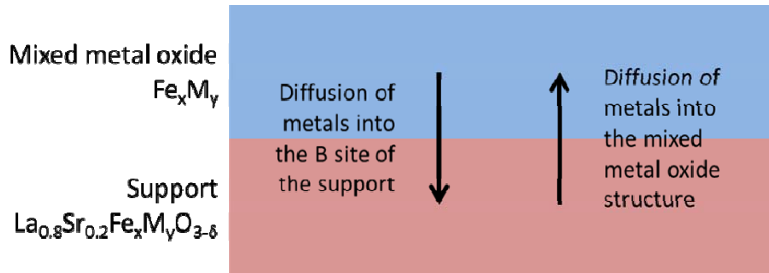Fixed mesh density for varying super cell sizes:

Orthorhombic CaMnO3: 4x4x4 for 1 unit cell; monkhorst pack

Orthorhombic Ca.75Sr.25MnO3: 4x4x4 for 1 unit cell; monkhorst pack

Hexagonal BaMnO3: 4x4x4 for 1 unit cell; Gamma centered

$$E_{O_V} = E_{AMnO_{3-\delta}} + \frac{1}{2} E_{O_2} - E_{AMnO_3}$$

Spinel/Bixbyite – Perovskite Phase Compatibility Studies

Mixed metal oxide Fe_xM_y

Support $La_{0.8}Sr_{0.2}Fe_xM_yO_{3-\delta}$

Diffusion of metals into the B site of the support

Diffusion of metals into the mixed metal oxide structure
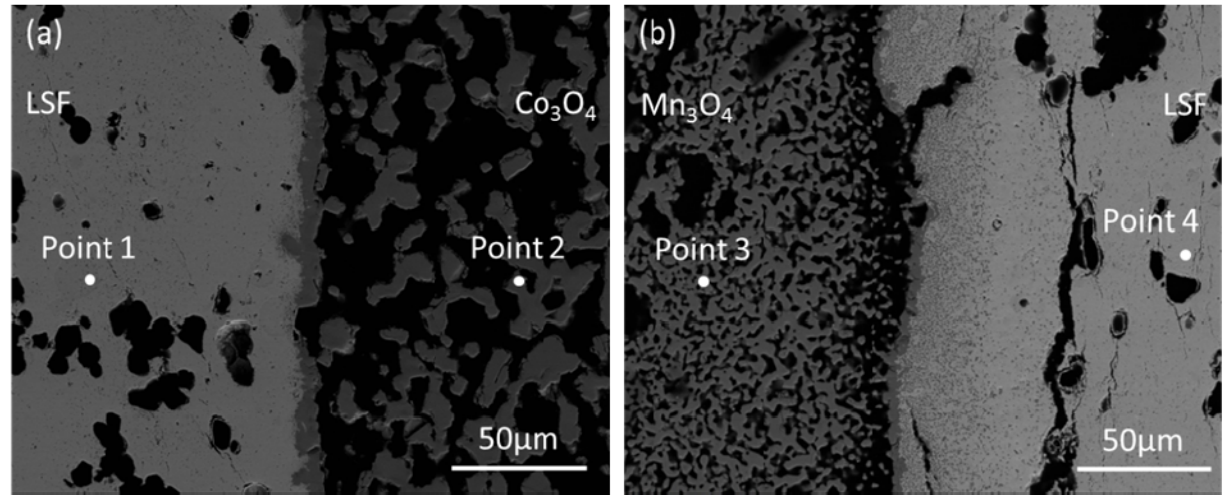
- *Sharp concentration differences when passing the phase boundary confirms that no significant phase diffusion is occurred and Co tends to stay in the mixed metal oxide part*

- *Gradual decrease in concentration of Mn when passing the phase boundary implies that manganese diffused through the LSF support and substitute iron in its B-site*

Element	Atomic % from EDX			
	Point 1	Point 2	Point 3	Point 4
Co or Mn	2.39	98.80	99.50	4.64
Fe	60.55	1.13	0.46	57.93
La	29.07	0.01	0.00	27.36
Sr	7.99	0.06	0.03	10.06

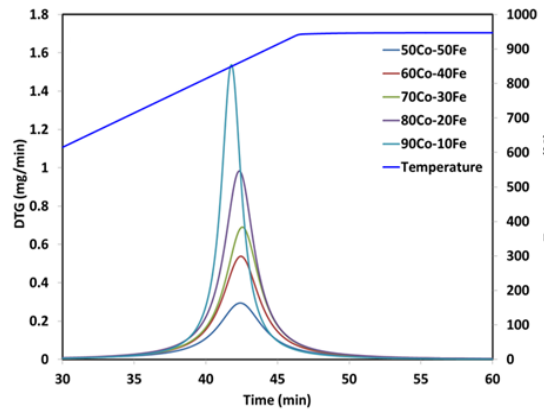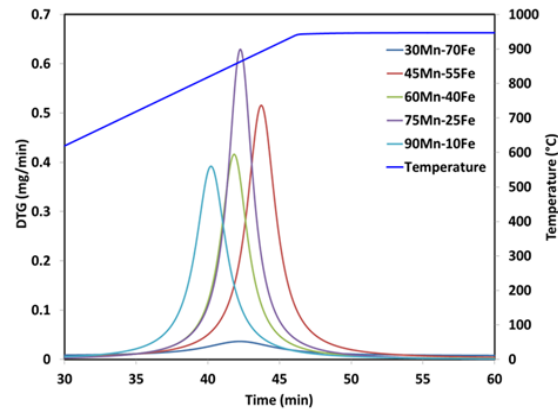# Metal Oxide Decomposition Behavior

Co-Fe oxide
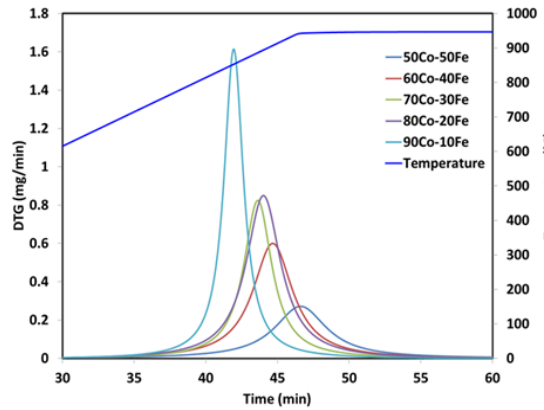
Mn-Fe oxide
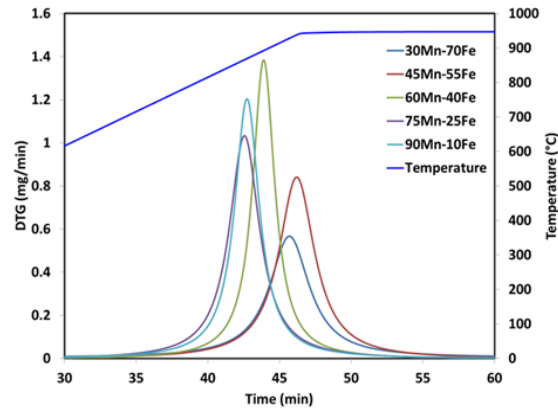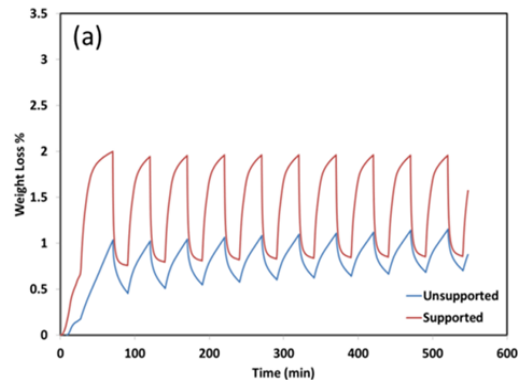
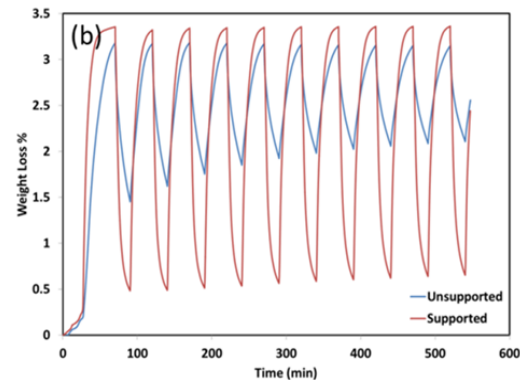**Co-Fe oxide
+
LSCF Support**

**Mn-Fe oxide
+
LSMF Support**

*Decomposition temperature of Co-Fe and Mn-Fe oxides decrease with decreasing Fe content.
Supported samples do not exhibit clear trends.*
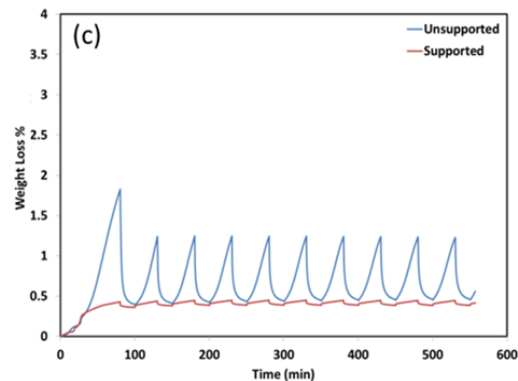
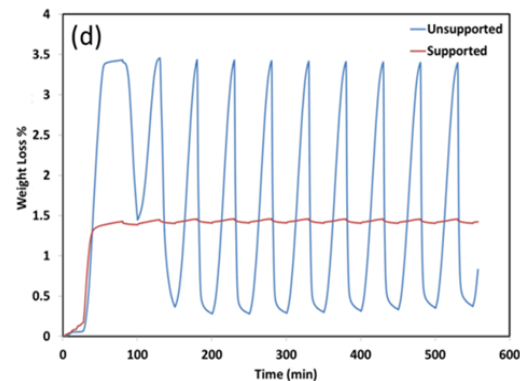# Isothermal CLOU Testing (850 ˚C, He inert ⬅➡ 10% O$_2$)
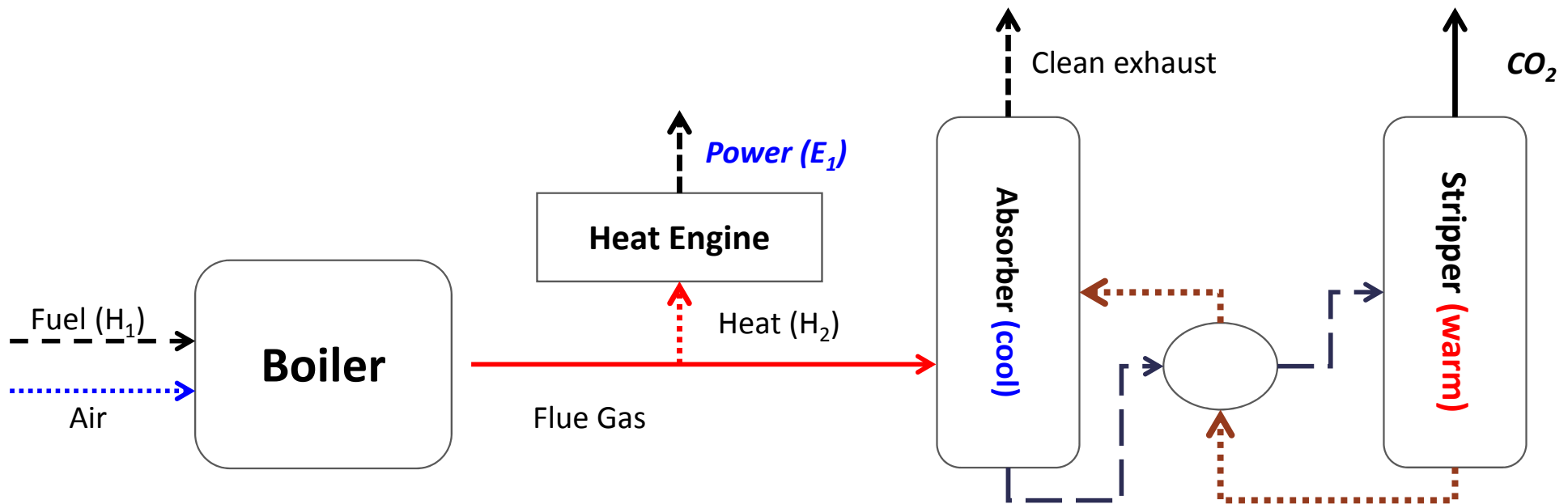
50% Co – 50% Fe

80% Co – 20% Fe

30% Mn – 70% Fe

60% Mn – 40% Fe

- *CLOU properties of mixed Fe-Co oxides are enhanced by perovskite addition*
- *Oxygen carrying capacity of mixed Fe-Mn oxides under an isothermal condition is negatively affected by perovskite addition*

# Why Chemical Looping: Conventional Post-Combustion CO_2 Capture

Limitations to conventional combustion – absorption based processes:
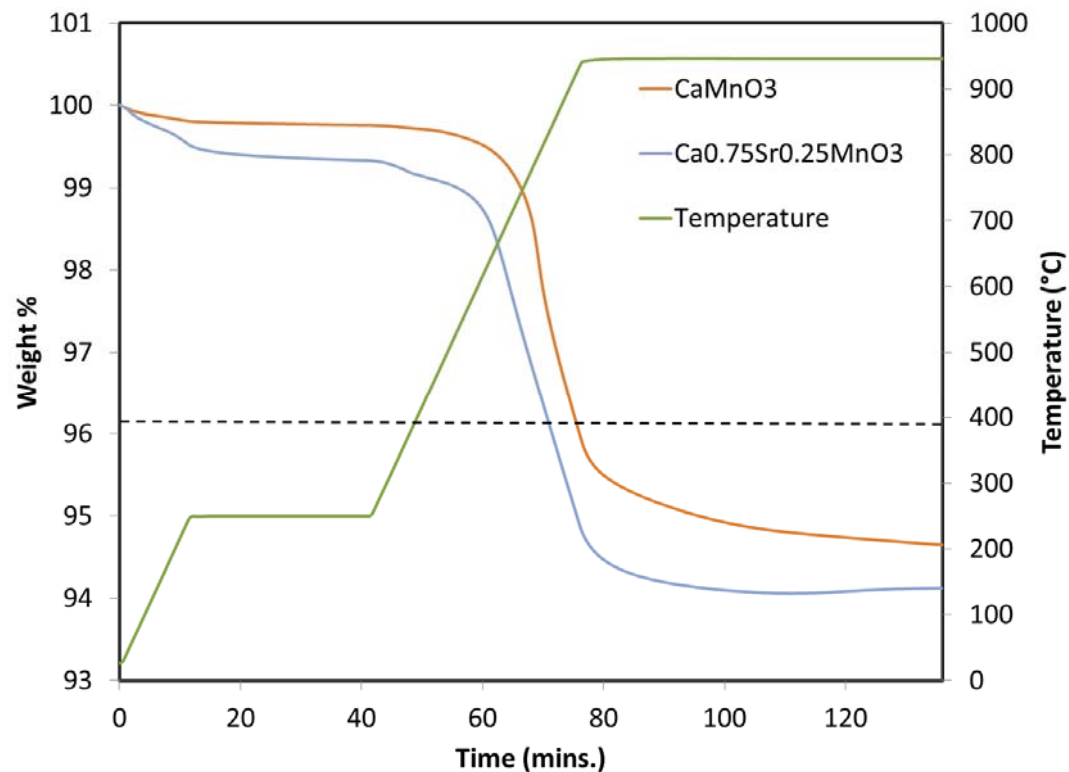
- Fixed extractible enthalpy from boiler/flue gas
- Absorber-stripper cycle consumes high grade heat and rejects low grade heat
- Delivery pressure of CO_2 is limited

Low 2nd Law efficiency!

DFT Investigation: $\Delta E_{vacancy}$ (Orthorhombic $CaMnO_3$)

Type 1 Vacancy Formation

Type 2 Vacancy Formation
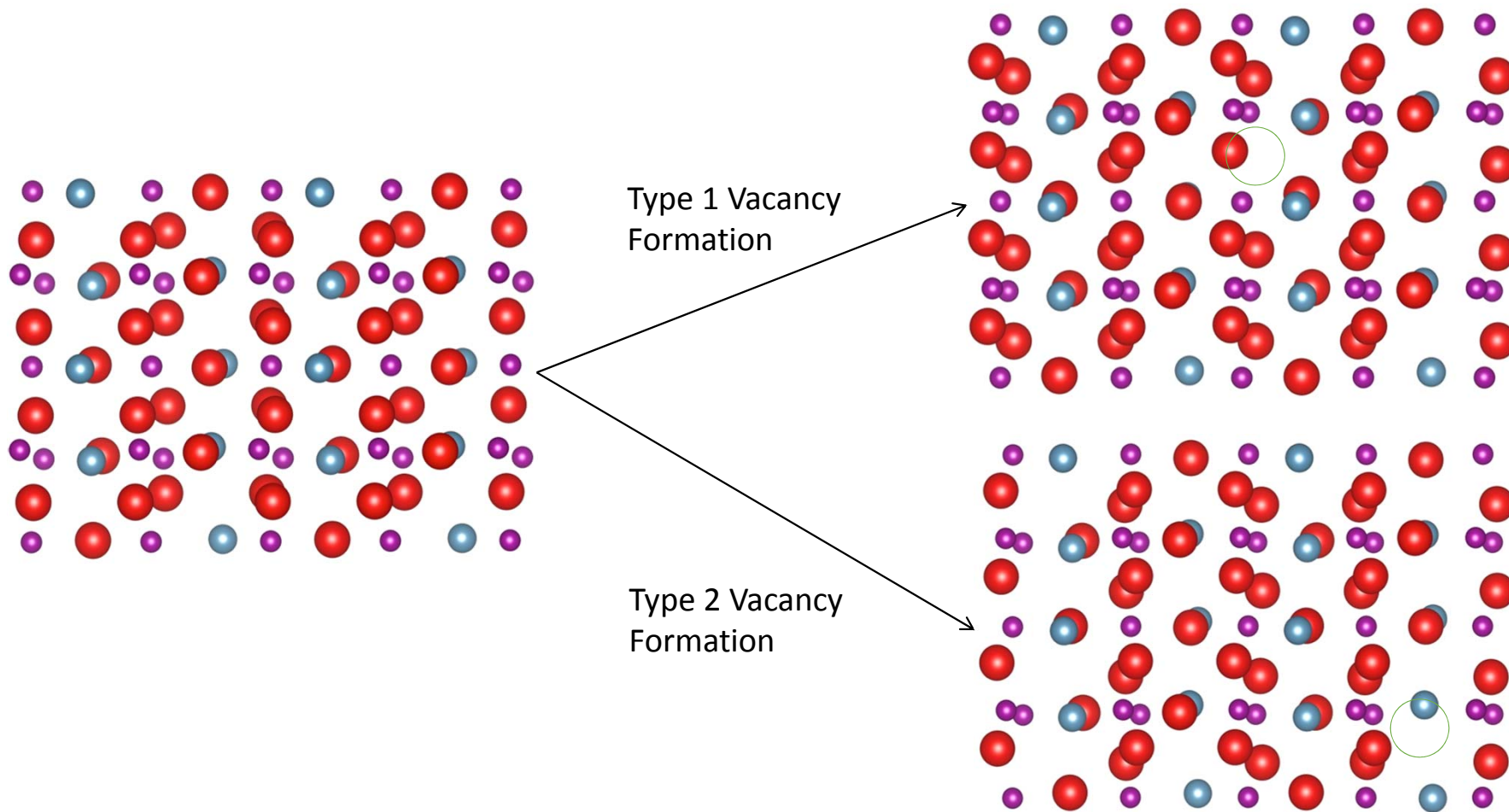
Char Oxidation using Perovskites

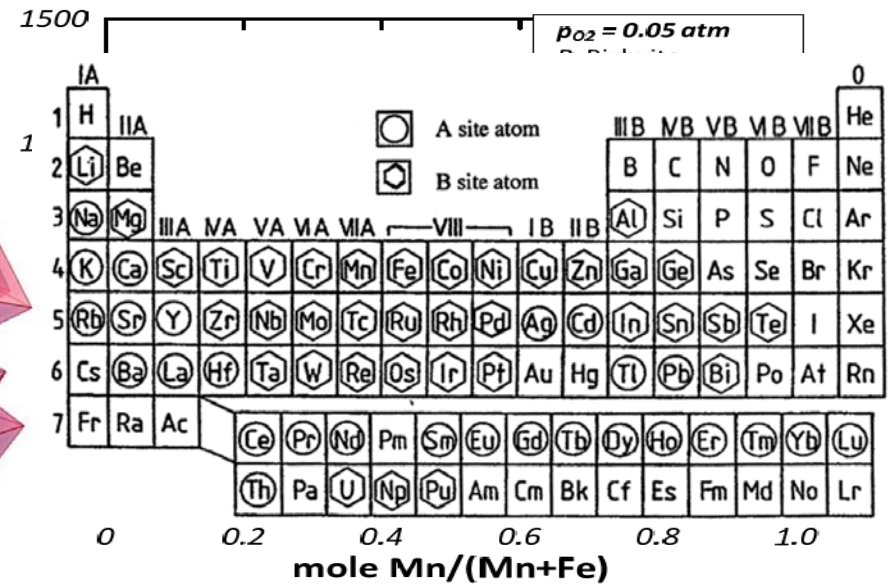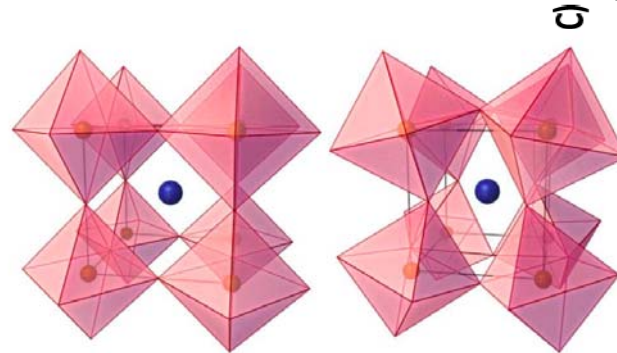

Sr doped perovskite shows notably lower reaction temperatures for char oxidation

Material Selection – Rapidly Expanding Material Design Space
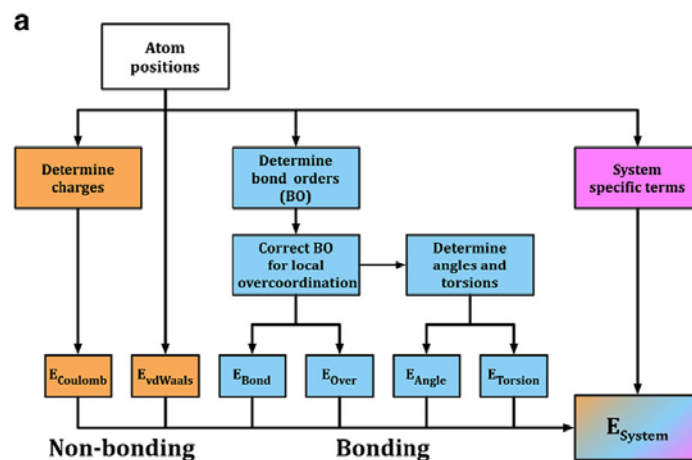
oxygen carrier material selections

- Iron
- Copper
- Manganese
- Nickel
- Cobalt
- Perovskite materials
- Mixed first row transition metal oxides

NC STATE UNIVERSITY

Reactive force field (ReaxFF)

- ReaxFF is a continuous bond order force field
- Force field parameters are developed by fitting to electronic structure calculations for the system of interest.
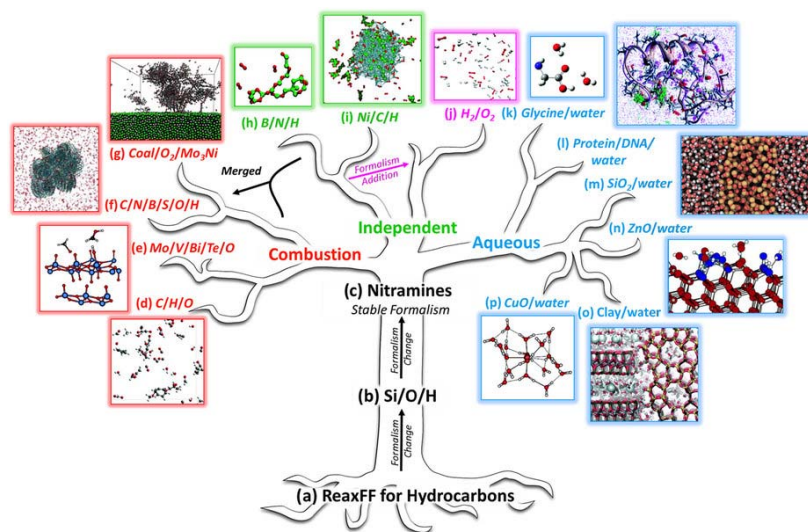

$$E_{system}=E_{bond}+E_{over}+E_{angle}+E_{tors}+E_{vdWaals}+E_{coulomb}+E_{specific}$$

$$BO_{ij}^{'} = BO_{ij}^{\sigma} + BO_{ij}^{\pi} + BO_{ij}^{\pi\pi} = \exp\left[p_{bo1} \cdot \left(\frac{r_{ij}}{r_o^{\sigma}}\right)^{p_{bo2}} \right] + \exp\left[p_{bo3} \cdot \left(\frac{r_{ij}}{r_o^{\pi}}\right)^{p_{bo4}} \right] + \exp\left[p_{bo5} \cdot \left(\frac{r_{ij}}{r_o^{\pi\pi}}\right)^{p_{bo6}} \right]$$

T. P. Senftle … A. van Duin Nat. Comp. Mater. 2016

Reactive force field (ReaxFF)

- ReaxFF is a continuous bond order force field
- ReaxFF has been applied to a wide variety of applications
- Force field parameters are dependent on the systems used to fit them
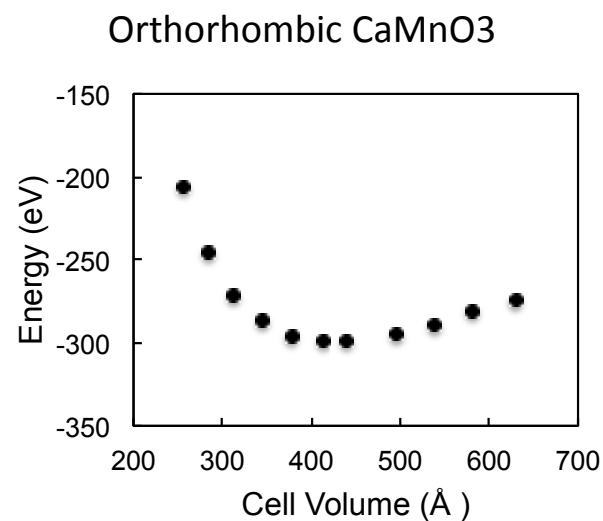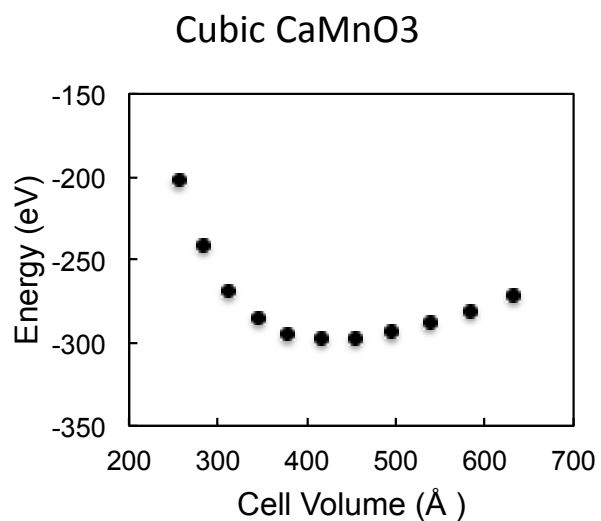- Parameters do not exists for all combinations of atoms

T. P. Senftle ... A. van Duin Nat. Comp. Mater. 2016

Building a training set for CaMnO$_3$

Crystal 'phase diagrams' from DFT calculations

Cubic CaMnO3

Orthorhombic CaMnO3

Still in progress …